

**MEDICAL IMAGE DENOISING USING
CONTOURLET
TRANSFORM, BILATERAL AND NLM
FILTERING**

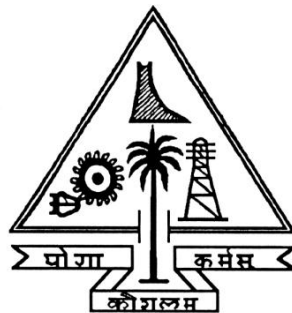
A thesis submitted in partial fulfillment of the requirements for the award of

**MASTER OF TECHNOLOGY
IN
COMMUNICATION ENGINEERING AND SIGNAL
PROCESSING**

of the Calicut University

by

MAHESH MOHAN M R
(Reg No. ETALCSP005)



**DEPARTMENT OF ELECTRONICS AND
COMMUNICATION ENGINEERING**
Govt. Engineering College Trichur Thrissur,
Kerala State, PIN 680 009

JULY 2013

CONTENTS

DECLARATION	iii
ACKNOWLEDEMENT	iv
ABSTRACT	v
CONTENTS	vi
LIST OF FIGURES	viii
LIST OF TABLES	x
LIST OF ABBREVIATIONS	xi
1. INTRODUCTION	1
1.1. OVERVIEW OF MEDICAL IMAGE NOISE	1
1.2. MOTIVATION	2
1.3. CHALLENGES	2
1.4. OBJECTIVE OF THE THESIS	3
1.5. ORGANISATION OF THE THESIS	3
1.6. CONTRIBUTION OF THE THESIS	4
2. LITERATURE SURVEY	5
3. PRELIMINARIES	12
3.1. DIGITAL IMAGE	12
3.2. IMAGE NOISE	13
3.3. IMAGE QUALITY METRIC FOR DENOISING	14
3.4. IMAGE DENOISING PLATFORM	15
3.5. CONCLUSION	16
4. SPATIAL DOMAIN DENOISING APPROACH	17
4.1. SPATIAL DOMAIN PROCESSING	17
4.2. MEAN FILTER	18
4.3. MEDIAN FILTER	19
4.4. BILATERAL FILTERING	20
4.5. NON LOCAL MEAN FILTER	22
4.6. RESULT ANALYSIS OF SPATIAL DOMAIN DENOISING	23
4.7. CONCLUSION	24

5. TRANSFORM DOMAIN DENOISING	25
5.1. DISCRETE COSINE TRANSFORM	25
5.1.1. Properties Of DCT	26
5.1.2. Medical Image Denoising Using Dct Transform	28
5.2. DISCRETE WAVELET TRANSFORM	29
5.2.1. Medical Image Denoising By Wavelet Shrinkage	33
5.3. CONTOURLET TRANSFORM	35
5.3.1. Frequency Domain View Of Image	36
5.3.2. Construction Of Contourlet Transform	38
5.3.3. Medical Image Denoising By Contourlet Shrinkage	39
5.4. RESULT ANALYSIS OF SPATIAL DOMAIN DENOISING	40
5.5. CONCLUSION	41
6. PROPOSED WORK AND RESULTS	42
6.1. INTRODUCTION	42
6.2. NOVEL WAVELET THRESHOLDING SCHEME	42
6.3. NOVEL CONTOURLET THRESHOLDING SCHEME	43
6.4. PROPOSED MEDICAL IMAGE DENOISING ENTITY	44
6.5. PROPOSED NATURAL IMAGE DENOISING ENTITY	44
6.6. SIMULATION RESULTS	45
7. CONCLUSION AND FUTURE PROSPECTS	49
REFERENCES	51

LIST OF FIGURES

Figures	page no.
Figure 3.1 Gaussian noise Image(mean 0,variance 0.05)	14
Figure 3.2 Gaussian noise Image(mean 0.5,variance 10)	14
Figure 3.3 Image denoising platform	15
Figure 3.4 Test images	16
Figure 4.1. Result of mean filter	18
Figure 4.2. Concept of mean filter	19
Figure 4.3. Concept of median filtering	19
Figure 4.4. Result of median filter	20
Figure 4.5. Result of bilateral filter	21
Figure 4.6. Result of NLM filter	23
Figure 4.6. Comparing performance of spatial domain techniques	23
Figure 5.1. Decorrelation property	27
Figure 5.2. Energy compaction property	27
Figure 5.3. Result of DCT denoising	29
Figure 5.4. Concept of wavelet transform(two basis set)	30
Figure 5.5. Concept of wavelet transform(three basis set)	31
Figure 5.6. Implementation of wavelet transform(three basis set)	31
Figure 5.7. Implementation of 2-D wavelet transform	32
Figure 5.8. 2-D wavelet transform subimage	32
Figure 5.9. Hard thresholding	33
Figure 5.10. Soft thresholding	34
Figure 5.11. Result of wavelet visushrink	35

Figure 5.12. Frequency representation showing directional features	36
Figure 5.13. Frequency representation showing intensity	37
Figure 5.14. Frequency representation showing low and high frequency	37
Figure 5.15. Directional filters having 2,4 and 8 bands resp.	38
Figure 5.16. Laplacian pyramid bands	38
Figure 5.17. Construction of Contourlet transform	39
Figure 5.18. Result of contourlet thresholding	39
Figure 5.19. Comparing performance of frequency domain techniques.	40
Figure 6.1. Proposed medical image denoising entity	44
Figure 6.2. Proposed natural image denoising entity	45
Figure 6.3. Comparing threshold performance	46
Figure 6.4. Comparing performance of medical image denoising	47
Figure 6.5. Comparing performance of natural image denoising	48

LIST OF TABLES

Tables	page no.
Table 4.1. Comparing performance of spatial domain techniques.	24
Table 5.1. Comparing performance of transform domain techniques.	40
Table 6.1. Comparison of PSNR of different thresholding schemes	46
Table 6.2. Comparison of PSNR of different denoising entities	47
Table 6.3. Comparison of processing time of different entities	48

LIST OF ABBREVIATIONS

Abbreviations

1. <i>AWGN</i>	Additive White Gaussian Noise
2. <i>DCT</i>	Discrete Cosine Transform
3. <i>CWT</i>	Continuous Wavelet Transform
4. <i>DWT</i>	Discrete Wavelet Transform
5. <i>LL</i>	Low-Low
6. <i>LH</i>	Low-High
7. <i>HL</i>	High-Low
8. <i>HH</i>	High-High
9. <i>PSNR</i>	Peak Signal to Noise Ratio
10. <i>MSE</i>	<i>Mean Square Error</i>
11. <i>AMF</i>	Adaptive Median Filter
12. <i>TV</i>	Total Variation
13. <i>NLm</i>	Non Local mean
14. <i>GGD</i>	Generalized Gaussian Distribution
15. <i>ICA</i>	Independent Component Analysis.
16. <i>GMM</i>	Gaussian Mixture Model
17. <i>MRI</i>	Magnetic Resonance Imaging
18. <i>CT</i>	Computer Tomography
19. <i>DTI</i>	Diffusion Tensor Imaging
20. <i>HARDI</i>	High Angular Resolution Diffusion Imaging

DECLARATION

I hereby declare that this submission is my own work and that, to the best of my knowledge and belief, it contains no material previously published or written by another person nor material which has been accepted for the award of any other degree or diploma of the university or other institute of higher learning, except where due acknowledgement has been made in the text.

Place:Trissur

Date:08-08-2013

Signature:

Name: Mahesh Mohan M R

Reg. No.:ETALCSP005

ACKNOWLEDGMENT

First of all I would like to thank the Sovereign Almighty who is taking care of me always and whose blessings have helped me to follow my dreams.

I would like to thank **Dr Sheeba.V.S**, my project guide for her assistance and constant support during my project work. She came up with the very initial idea of denoising in medical field. I greatly appreciate her invaluable guidance, which helped me complete this thesis.

I express my sincere thanks to **Mrs Muneera.C.R, Mrs Latha K.N, Mr Premanand.B** for their cooperation, guidance and invaluable support for preparing and presenting this paper. My sincere gratitude to all the faculty and staff of the Department of Electronics and Communication Engineering GEC Thrissur.

Special thanks to all my mentors in my lifetime. I thank my parents and my sister, for their support and guidance, which gave me an opportunity to pursue higher studies.

Last but not the least I would like to thank all my friends whose support was very valuable during my Master's study at GEC Thrissur.

MAHESH MOHAN M R

I. ABSTRACT

In medical imaging if the SNR is too small it becomes very difficult to detect anatomical structures. To obtain a high SNR image without lengthy repeated scans, post-processing of data such as denoising plays a critical role.

Wavelet universal thresholding yields overly smoothed images. Contourlet transform which is much better than the wavelet transform in conserving edges and line details is inferior for medical image denoising compared to wavelet thresholding.

Bilateral filtering is one of the commonly used procedures for medical image denoising. As an extension of bilateral filtering Non-Local means (NLm) image denoising have been introduced which utilizes structural similarity. However bilateral and NLm filtering does not give satisfactory results since real gray levels are polluted seriously by noise.

As the wavelet universal thresholding is an estimate which is asymptotically optimal, a novel scaling parameter is empirically introduced to the universal threshold. Also this idea has been extended to contourlet transformation Finally a novel single entity for medical image denoising is been devised comprising of proposed contourlet thresholding and NLm filtering. A natural image denoising entity is also been proposed using proposed contourlet thresholding and bilateral filtering.

These new entities have been tested with various noisy medical images, including MRI image of human brain and CT image of Abdomen. Simulation results show that the proposed method is superior compared to existing medical image denoising scheme using Bilateral or NLm filtering.

CHAPTER 1

INTRODUCTION

1.1 OVERVIEW OF MEDICAL IMAGE NOISE

Digital images play an important role both in daily life applications such as medical imaging, satellite television, magnetic resonance imaging, computed tomography as well as in areas of research and technology such as geographical information systems and astronomy. Data sets collected by medical image sensors are generally contaminated by noise. Noise is often defined as the uncertainty in a signal due to random fluctuations in that signal. Noisy image can be caused by a transient during image acquisition, a faulty sensor in a camera, a faulty memory, compression and noise in a channel during transmission. As a result, the values of some pixels are changed. The amount of noise (or noise density) of a noisy image depends on a number of factors including image acquisition environments, quality of equipment, and channel conditions. However, the incorporated noise during image acquisition degrades the human interpretation, or computer-aided analysis of the images.

In medical imaging usually we face a relatively low SNR with good contrast, or a low contrast with good SNR. Fortunately the human visual system is highly effective in recognizing structures even in the presence of a considerable amount of noise. But if the SNR is too small or the contrast too low it becomes very difficult to detect anatomical structures because tissue characterization fails. A definition of overall image quality depends on specific diagnostic tasks. In some cases a high spatial resolution and a high contrast are required, whereas in other cases more perceptual criteria may be favored. For a visual analysis of medical images, the clarity of details which mainly comprises edge information and the object visibility are important.

In general, there are two approaches to reduce noise in a medical image. The first approach is to acquire a second image which results in a longer acquisition time and an increased cost. The second approach is to apply some image post-processing technique referred as image denoising, to reduce the noise in an acquired image which usually requires less time and can

reduce cost. For the ease of detection of illness as fast as possible and the reduced expenditure for medical diagnosis, second approach is usually preferred.

1.2 MOTIVATION

The rapid development of advanced medical imaging technologies such as Magnetic Resonance Imaging(MRI), Positron Emitted Tomography (PET) and Computer Tomography (CT) have provided us an unprecedented way to diagnose illness in-vivo and non-invasively. Some of the most advanced techniques based on this imaging modality remain in the research stage but never reach routine clinical usage. One of the bottlenecks is due to low Signal-to-Noise Ratio (SNR) which requires long and repeated acquisition of the same subject to reduce noise and blur. For example, a high SNR Diffusion Tensor Imaging (DTI) dataset requires an hour of data acquisition[1]. A high SNR of High-Angular-Resolution Diffusion Imaging (HARDI) data can take 13 hours [2]. To recover high SNR image from noisy and blurry image without lengthy repeated scans, post-processing of data plays a critical role in two aspects: (1) automatic denoising and deblurring algorithms can restore the data computationally to achieve a quality that might take much longer otherwise. (2) Computational object segmentation techniques can perform intelligent extraction of data directly and automatically from noisy observations.

While providing access to important new anatomical and functional information through high-speed acquisition, or high spatial resolution, advanced imaging techniques are often penalized by a decrease in image SNR. In addition to these blurring effects, the recorded image is corrupted by noises too. Each element in the imaging chain such as lenses, film, digitizer, etc. contribute to the degradation. Thus, denoising is often a necessary and the first step to be taken before the images data is analyzed. It is necessary to apply an efficient denoising technique to compensate for such data corruption.

1.3 CHALLENGES

Noise suppression in medical images is a particularly delicate and difficult task. A trade-off between noise reduction and the preservation of actual image features has to be made in a way that enhances the diagnostically relevant image content.

The goal of image denoising methods is to recover the original image from a noisy measurement,

$$v(i, j) = u(i, j) + n(i, j) \quad (1)$$

where $v(i, j)$ is the observed image, $u(i, j)$ is the “true” image and $n(i, j)$ is the noise perturbation at a pixel (i, j) . The denoising methods should find $u(i, j)$ from $v(i, j)$ in the unaltered form. The main point is that the actual intensities of both $u(i, j)$ and $n(i, j)$ are unknown to us, and when this problem is solved without any additional knowledge it is referred to as blind denoising. These types of problems are generally considered hard to solve as illustrated by the fact that there are literally infinitely many ways to decompose a signal into the sum of two components. Therefore, in order to find a unique solution, various conditions need to be imposed on each of the two components. The best simple way to model the effect of noise on a digital image is to add a gaussian white noise. In that case, $n(i, j)$ are i.i.d gaussian values with zero mean and variance σ^2 . But problem is that most denoising methods degrade or remove the fine details and texture of $u(i, j)$.

1.4 OBJECTIVE OF THE THESIS

The goal of this thesis is to introduce a novel medical image denoising approach focusing on the implementation of high performance algorithm compared to currently prevailing techniques. Since it is difficult (in terms of time and cost) to completely alter the prevailing medical image denoising software algorithm, a preprocessing step need to be added to the existing technique. NLm denoising and bilateral filtering, currently used techniques are being experimented with and added a preprocessing step to enhance its performance. In this thesis denoising entities are proposed under the constraint of less processing time since less processing time is a crucial feature for medical image denoising.

1.5 ORGANISATION OF THE THESIS

A novel method of Medical image denoising using Contourlet transform, bilateral and NLm filtering is the crux of this thesis. Chapter 2 discusses the literature review undergone. Chapter 3 describes basic preliminaries which set the stage for development over further chapters. Chapter 4 gives a review about the existing spatial domain denoising techniques including commonly used bilateral and NLm filtering. In Chapter 5, transform domain denoising techniques using Discrete cosine transform (DCT), Discrete Wavelet Transform (DWT) and Contourlet transform are discussed. Chapter 6 discusses the proposed novel medical image denoising entity and the proposed natural image denoising entity and the performance evaluation of the denoising scheme. Chapter 7 concludes the thesis with a future prospects.

1.6 CONTRIBUTION OF THE THESIS

In this thesis a novel technique of denoising to medical images corrupted by AWGN is proposed.

This thesis puts forward four contributions

- 1) As the universal thresholding is an estimate which is asymptotically optimal in the minmax sense, a scaling parameter is introduced to the universal threshold by extensive simulation and regression of data with wide range of standard medical images as well as natural images of different size and corrupted by different noise variances.
- 2) This idea has been extended to contourlet transformation with a new scaling factor and the same universal thresholding.
- 3) A novel medical image denoising entity is introduced using proposed contourlet thresholding as a pre-processing step prior to NLm filtering. It can give significant improvement in PSNR as well as visual quality from bilateral and NLm filter used alone.
- 4) As a by-product of medical image denoising work, a novel entity is been introduced suitable for natural image denoising comprised of proposed contourlet thresholding and bilateral filtering.

CHAPTER 2

LITERATURE SURVEY

Noise introduced in an image is usually classified as substitutive (impulsive noise: e.g., salt & pepper noise, random-valued impulse noise, etc.) and additive (e.g., additive white Gaussian noise) noise. The impulsive noise of low and moderate noise densities can be removed easily by simple denoising schemes available in the literature.

In many occasions, noise in digital images is found to be additive white Gaussian noise (AWGN) with uniform power in the whole bandwidth and with Gaussian probability distribution. Traditionally, AWGN is suppressed using linear spatial domain filters such as Mean filter, Wiener filter [3,4,5], etc. The spatial mean filters are a simple sliding window filter that replaces the center value by the calculated mean value. Linear techniques possess mathematical simplicity but have the disadvantage of yielding blurring effect. They also do not perform well in the presence of signal dependent noise. An adaptive standard recursive low pass filter is designed by Klaus Rank and Rolf Unbehauen [6] considered the three local image features edge, spot and flats as adaptive regions with Gaussian noise. Inherently noise removal from image using linear filtering introduces blurring in many cases.

Nonlinear filters [5] are then developed to avoid the aforementioned disadvantages. Non-linear filters control the direction and/or degree of averaging with the local contents of neighborhood because the spatial relations of the gray values of neighborhood pixels can recognize the objects in an image. The well-known nonlinear filter is median filter. Median filter has been introduced by Tukey [7] in 1970. Median filter now is broadly used in reducing noise and smoothing the images. The problem of simple median filter is that, it works nicely only for suppressing impulsive noise of low density. Hakan et al., [8] have used topological median filter to improve conventional median filter. The better performance of the topological median filters over conventional median filters is in maintaining edge sharpness.

Yanchun et al., [9] proposed an algorithm for image denoising based on Average filter with maximization and minimization for the smooth regions, unidirectional Median filter for edge region and median filter for the indefinite region. It was discovered that when the image is corrupted by both Gaussian and impulse noises, neither Average filter nor Median filter algorithm will obtain a result good enough to filter the noises from medical images because of the complexity of their algorithm.

The Adaptive Median Filter (AMF) [10] is another non-linear filter to reduce the noise by using varying window size and increases the size of the window is increased until correct value of median is calculated and noise pixel is replaced with its calculated median value. Here two conditions are used, one condition is used to detect the corrupted pixels and second one is used to check the correctness of median value. If trial pixel is less than minimum value present in rest of pixel in window and if text pixel is greater than maximum value present in rest of pixel in window than center pixel then it is treated as corrupted pixel. If calculated median is corrupted then increase the window size and recalculate the median value until we get correct median value or else window size reach maximum limit.

One of the branches for the improvement of median filter is based on switching approach [11]. In general, switching median filter divides its implementation into two stages; which are noise revealing stage, and noise annulment stage. During the first stage, by using some of the image characteristics such as pixel intensity, the noise discover algorithms classify the image pixels either “noise” or “noise-gratis” pixels. Then, in the second stage of the method, only “noise” pixels are processed by the filter, whereas “noise-gratis” pixels are left unchanged. This condition enables the method to preserve most of the image details. Switching median filters identifies each pixel as “corrupted” or “original”, only those corrupted pixels would undergo the filtering process, while other pixels remain unchanged. So SM filter can get more satisfactory results for restraining impulse noise. The disadvantage of switching median filter is Less effective in removing Gaussian or random intensity noise. The median filter can remove noise only if the noisy pixels occupy less than one half of the neighborhood area.

Progressive switching median filter is a median based filter [12], which works in two stages. In the first stage an impulse detection algorithm is used to generate a sequence of binary flag images. This binary flag image predicts the location of noise in the observed image. In the second stage noise filtering is applied progressively through several iterations. This filter is a very

good filter for fixed valued impulsive noise but for random values the performance is abysmal. The advantage of using progressive switching median filter is that it preserves the positions of boundaries in an image, making this method useful for visual examination and measurement. But the disadvantage is that it removes both the noise and the fine detail since it can't tell the difference between the two.

Total variation (TV) regularization is a technique that was originally developed for AWGN image denoising by Rudin, Osher, and Fatemi [13]. The TV regularization technique has since been applied to a multitude of other medical imaging problems. It filters out noise by reducing the total variation of image, while preserving edges. The problem is that, the process is iterative so that computational cost and time of processing is very high.

When developing a filtering method for medical image data, image degradation by blurring or by artifacts resulting from a filtering scheme is not acceptable. The following criterias should ideally be fulfilled:

- 1) Minimize information loss by preserving object boundaries and detailed structures.
- 2) Efficiently remove noise in regions of homogeneous physical properties.

Recent developments based on bilateral filtering[14,15] overcome the major drawbacks of conventional spatial filtering, and significantly improve image quality while satisfying the main criteria 1 stated above. Bilateral filtering is one of the examples of non-linear non-iterative filtering. It combines domain and range filters simultaneously. It preserves edge information while denoising. However it does not give satisfactory results, real gray levels are polluted seriously and the range filter cannot work properly. This would lead to bring side effect to the denoising results like a polishing look to denoised image. For example, image's tissue regions (especially small structural details and the distinct edge features may be weakened).This phenomenon is referred as propagation of noise (PoN) .

The switching bilateral filter [16] proposed by C. H. Lin et al, is a nonlinear filter which removes both Gaussian and impulse noise while preserving image details. This filter consists of two stages, in first stage to identify the type of noise and second stage is to apply the filtering to the noisy pixel. A Modified Switching Bilateral filter, which is supported by the global trimmed mean value instead of reference median value and the weights of the bilateral filter is supported by the noise free pixels alone. But, in bilateral and switching bilateral filters, weights depend on both

noisy and noise gratis pixels in the window. The modified switching bilateral filtering removes the noise and enhances the fine details in an image, by means of a nonlinear combination of nearby noise free pixel and global trimmed mean value. The main disadvantage of Bilateral filter is its complexity.

As an extension of bilateral filtering, Buades et al. had put forward Non-Local means image denoising [17,18] which utilizes structural similarity .Generally speaking, the information in a natural image is redundant to some extent. Based on this observation, Buades developed a NL means image denoising algorithm which takes full advantage of image redundancy. The basic idea is that images contain repeated structures, and averaging them will reduce the (random) noise. It is an efficient denoising method with the ability to result in proper restoration of the slowly varying signals in homogeneous tissue regions while strongly preserving the tissue boundaries. The drawback of NLM filter is that a single pixel with a very unrepresentative value can significantly affect the mean value of all the pixels in its neighbourhood. When the filter neighbourhood bestride an edge, the filter will interrupt new values for pixels on the edge and so will blur that edge. This produces a problem if sharp edges are required in the output. So the NLM filter may suffer from potential limitations since the calculation for similarity weights is performed in a full-space of neighbourhood. Specifically, the accuracy of the similarity weights will be affected by noise.

Anisotropic diffusion [19] is also a powerful filter where local image variation is measured at every point, and pixel values are averaged from neighbourhoods whose size and shape depend on local variation. Diffusion methods average over extended regions by solving partial differential equations, and are therefore inherently iterative. More iteration may lead to instability where, in addition to edges, noise becomes prominent.

In transform domain Qingling Sun[20] proposed denoising in DCT domain, which is found to be superior to denoising in spatial domain, but still sacrifices edge and texture details.

Now-a-days, wavelet transform is employed as a powerful tool for image denoising [4,21]. Image denoising using wavelet techniques is effective because of its ability to capture most of the energy of a signal in a few significant transform coefficients, when natural image is corrupted with Gaussian noise. Another reason of using wavelet transform is due to development of efficient algorithms for signal decomposition and reconstruction for image processing

applications such as denoising and compression. Many wavelet-domain techniques are already available in the literature. Out of various techniques soft-thresholding proposed by Donoho and Johnstone [22] is most popular. The use of universal threshold to denoise images in wavelet domain is known as VisuShrink .

More recently, wavelet based filters have been applied successfully to MR image denoising [23,24,25]. Donoho and Johnstone have shown that VisuShrink results in an estimate asymptotically optimal in the minimax sense. When images are denoised by VisuShrink, in many cases VisuShrink can outperform the classic linear Wiener filtering, especially for the images with a low peak signal-to-noise ratio (PSNR). However; it is also well known that VisuShrink yields overly smoothed images. This is because its threshold choice can be unwarrantedly large due to its dependence on the number of samples. Although Donoho's concept was not revolutionary, his methods did not require tracking or correlation of the wavelet maxima and minima across the different scales as proposed by Mallat. Thus, there was a renewed interest in wavelet based denoising techniques since Donoho demonstrated a simple approach to a difficult problem. Researchers published different ways to compute the parameters for the thresholding of wavelet coefficients. Data adaptive thresholds [26] were introduced to achieve optimum value of threshold. The problem of finding adaptive threshold consumes more time thus adversely affecting medical image processing.

Donoho improved his work using the *SURE* threshold. It is subband adaptive and is derived by minimizing Stein's unbiased risk estimator. Recently, by modelling the wavelet coefficients within each subband as i.i.d random variables with generalized Gaussian distribution (GGD), Chang *et al.* [27] proposed the *BayesShrink* scheme. The *BayesShrink* threshold is also subband dependent and yields better results than the *SURE* threshold. The thresholds mentioned above are based on orthogonal wavelets and are *soft*, implying that the input is shrunk to zero by an amount of threshold.

In [28], Pan *et al.* presented a *hard* threshold with a nonorthogonal wavelet expansion. The word *hard* implies that the input is preserved if it is greater than the threshold; otherwise it is set to zero.

In the noise reduction technique of Pizurica [29], the interscale correlation information is exploited to classify the wavelet coefficients. The preliminary classification is then used to estimate the distribution of a coefficient to decide if it is a feature. If a coefficient at a coarser

scale has small magnitude, its descendant coefficients at finer scales are likely to be small. Shapiro exploited this property to develop the well-known embedded zero tree wavelet coder [30]. Conversely, if a wavelet coefficient produced by a true signal is of large magnitude at a finer scale, its parents at coarser scales are likely to be large as well. However, for those coefficients caused by noise, the magnitudes will decay rapidly along the scales. With this observation, Xu *et al.* [31] multiplied the adjacent wavelet scales to sharpen the important structures while weakening noise. They developed a spatially selective filtering technique by iteratively selecting edge pixels in the multiscale products.

Tan *et al.* [32] proposed a wavelet domain denoising algorithm by combining the expectation maximization scheme and the properties of the Gaussian scale mixture models. The algorithm is iterative in nature and the number of iterations depends on the noise variance. For high variance Gaussian noise, the method undergoes many iterations and therefore the method is computationally-intensive.

Statistical Modeling of Wavelet Coefficients focuses on some more interesting and appealing properties of the Wavelet Transform such as multiscale correlation between the wavelet coefficients, local correlation between neighbourhood coefficients etc. This approach has an inherent goal of perfecting the exact modelling of image data with use of Wavelet Transform.

The Gaussian mixture model (GMM) and the generalized Gaussian distribution (GGD) are commonly used to model the wavelet coefficients distribution. Although GGD is more accurate, GMM is simpler to use. In [33], authors proposed a methodology in which the wavelet coefficients are assumed to be conditionally independent zero-mean Gaussian random variables, with variances modelled as identically distributed, highly correlated random variables. An approximate Maximum A Posteriori (MAP) Probability rule is used to estimate marginal prior distribution of wavelet coefficient variances. All these methods mentioned above require a noise estimate, which may be difficult to obtain in practical applications.

F Russo [34] proposed a new method for automatic enhancement of noisy images. The most relevant feature of the proposed approach is a novel procedure for automatic tuning that takes into account the histograms of the edge gradients.

Recently a new method called Independent Component Analysis (ICA) has gained wide spread attention. The ICA method was successfully implemented in [35, 36] in denoising Non-Gaussian data. One exceptional merit of using ICA is its assumption of signal to be Non-

Gaussian which helps to denoise images with Non-Gaussian as well as Gaussian distribution. Drawbacks of ICA based methods as compared to wavelet based methods are the computational cost because it uses a sliding window and requires sample of noise free data or at least two image frames of the same scene. In some applications, it might be difficult to obtain the noise free training data.

Minh N. Do and Martin Vetterli put forward a new dimension in image transform named contourlet transform[37],which proved to be much better than the wavelet transform in conserving edges and line details. The improvement in approximation by contourlets based on keeping the most significant coefficients will directly lead to improvements in denoising,. As an example, for image denoising, random noise will generate significant wavelet coefficients just like true edges, but is less likely to generate significant contourlet coefficients. Consequently, a simple thresholding scheme applied on the contourlet transform is more effective in removing the noise than it is for the wavelet transform. The problem is that directly using the universal threshold which suites well in wavelet domain is not suitable in contourlet domain, since the number of elements in transform coefficients for contourlet is much higher than wavelet coefficients.

As the contourlet transform performs similar to wavelet transform with additional features of anisotropy and directionality, it is found to be better than wavelet in image denoising [38]. Atif Bin Mansoor[38] has proposed that visushrink performs better on contourlet transform for a small range of images because of its superiority as compared to wavelet transform.

But, none of the denoising algorithm available in literature is able to achieve perfect restoration. Further, there is a need to reduce computational complexity of a denoising algorithm for its use in real-time applications. Hence, it may be concluded that there is enough scope to develop better denoising schemes with very low computational complexity that may yield high noise reduction as well as preservation of edges and fine details in medical images.

CHAPTER 3

PRELIMINARIES

3.1 DIGITAL IMAGE

Digital media offer several distinct advantages over analog media: the quality of digital audio, images and video signals are higher than that of their analog counterparts. Editing is easy because one can access the exact discrete locations that should be changed. Copying is simple with no loss of fidelity. Additional advantages include: the ease with which they can be displayed on computer monitors, and their appearance modified at will; the ease with which they can be stored on, for example, CD-ROM or DVD; the ability to send them between computers, via the internet or via satellite; the option to compress them to save on storage space or reduce communication times. Many of these advantages are particularly relevant to medical imaging. Increasingly, hospitals are networking their digital imaging systems into so-called PACS (Picture and Archiving Systems), RIS/HIS (Radiological/Hospital Information Systems), which include patient diagnosis and billing details along with the images. A two dimensional digital image can be represented as a two dimensional array of data $u(i, j)$, where (i, j) represent the pixel location. The pixel value corresponds to the brightness of the image at location (i, j) . Some of the most frequently used image types are binary, gray-scale and color images [4,21].

Binary images are the simplest type of images and can take only two discrete values, black and white. Black is represented with the value '0' while white with '1'. Note that a binary image is generally created from a gray-scale image. A binary image finds applications in computer vision areas where the general shape or outline information of the image is needed. They are also referred to as one bit/pixel images. Gray-scale images are known as monochrome or one-color images. The images used for experimentation purposes in this thesis are all gray-scale images. They contain no color information. They represent the brightness of the image. This image contains eight bits/pixel data, which means it can have up to 256 (0-255) different brightness levels. A '0' represents black and '255' denotes white. In between values from 1 to 254 represent the different gray levels. As they contain the intensity information, they are also referred to as intensity images.

Color images are considered as three band monochrome images, where each band is of a different color. Each band provides the brightness information of the corresponding spectral band. Typical color images are red, green and blue images and are also referred to as RGB images. This is a 24 bits/pixel image.

3.2 IMAGE NOISE

Noise is undesired information that contaminates the image. In the image denoising process, information about the type of noise present in the original image plays a significant role. Typical images are corrupted with noise modeled with Gaussian distribution. Another typical noise is a speckle noise, which is multiplicative in nature and noise modelled with uniform, or salt and pepper distribution.

Noise is present in an image either in an additive or multiplicative form [4]. An additive noise follows the rule

$$v(i, j) = u(i, j) + n(i, j) \quad (3.1)$$

while the multiplicative noise satisfies

$$v(i, j) = u(i, j) \times n(i, j) \quad , \quad (3.2)$$

where $u(i, j)$ is the original signal, $n(i, j)$ denotes the noise introduced into the signal to produce the corrupted image $v(i, j)$, and (i, j) represents the pixel location. The above image algebra is done at pixel level. The digital image acquisition process converts an optical image into a continuous electrical signal that is then sampled. At every step in the process there are fluctuations caused by natural phenomena, adding a random value to the exact brightness value for a given pixel.

One of the general way to approximate the noise is Gaussian noise, which is evenly distributed over the entire image. This means that each pixel in the noisy image is the sum of the true pixel value and a random Gaussian distributed noise value. As the name indicates, this type of noise has a Gaussian distribution, which has a bell shaped probability distribution function given by,

$$F(g) = \frac{1}{\sqrt{2\pi\sigma^2}} e^{-(g-m)^2/2\sigma^2} \quad (2.3)$$

where g represents the gray level, m is the mean or average of the function, and σ^2 is the noise variance. When introduced into an image, Gaussian noise with zero mean and variance as 0.05 would look as in Fig 3.1. Fig 3.2 illustrates the Gaussian noise with mean as 1.5 and variance as 10 over a base image with a constant pixel value of 100.

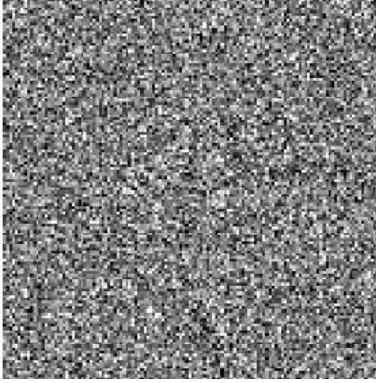


Fig 3.1: Gaussian noise Image
(mean=0, variance 0.05)

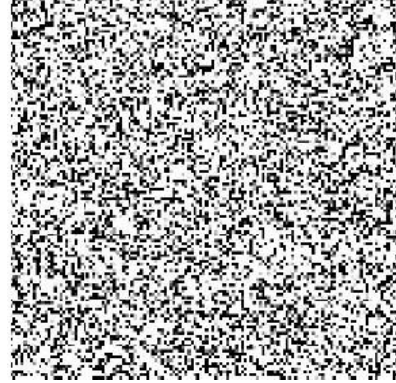


Fig 3.2: Gaussian noise Image
(mean=1.5, variance 10)

3.3 IMAGE QUALITY METRIC FOR DENOISING

The quality of an image is examined by objective evaluation as well as subjective evaluation. For subjective evaluation, the image has to be observed by a human expert. The human visual system (HVS) is so complicated that it is not yet modeled properly. Therefore, in addition to objective evaluation, the image must be observed by a human expert to judge its quality. There are various metrics used for objective evaluation of an image. Some of them are mean squared error (MSE), root mean squared error (RMSE) and peak signal to noise ratio (PSNR) [34].

$$v(i, j) = u(i, j) + n(i, j) \quad (3.4)$$

For the above additive noise process, let the original noise-free image, noisy image, and the denoise image be represented by $u(i, j)$, $v(i, j)$, and $\hat{u}(i, j)$ respectively. Here, (i, j) represent the discrete spatial coordinates of the digital images. Let the images be of size $M \times N$ pixels (i.e. $i=1,2,3,\dots,M$, and $j=1,2,3,\dots,N$). Then, MSE and RMSE are defined as:

$$MSE = \sum_{\substack{1 \leq i \leq M \\ 1 \leq j \leq N}} \frac{[\hat{u}(i, j) - u(i, j)]^2}{M \times N} \quad (3.5)$$

$$RMSE = \sqrt{MSE} \quad (3.6)$$

The PSNR is defined in logarithmic scale, in dB. It is a ratio of maximum signal power to noise power. Since the MSE represents the noise power and the peak signal power is MAX_i^2 , where MAX_i is the maximum pixel value of an image. For an 8 bit image MAX_i is equal to 255.

$$PSNR = 10 \log_{10} \frac{MAX_i^2}{MSE} dB \quad (3.7)$$

These measures, as such, do not represent human perception of the images, i.e. visual quality of the images. It is very difficult to gauge denoised images mathematically on visual quality as human vision system is not only highly subjective but also exhibit different tolerance levels to various types of noises. Thus authentication of denoising method requires both quantitative measure and qualitative inspection of image[34]. In this thesis, both criterias are applied; first the PSNR and then the image is also viewed for visual acceptance.

3.4 IMAGE DENOISING PLATFORM

There are various methods to help restore an image from noisy distortions. Selecting the appropriate method plays a major role in getting the desired image. The denoising methods tend to be problem specific. For example, a method that is used to denoise satellite images may not be suitable for denoising medical images. In this thesis, a study is made on the various medical image denoising algorithms and each is implemented in Matlab 7.6. Also a novel method has been proposed, which shown to be outperform the existing denoising methods. Each method is compared and classified in terms of its efficiency.

In case of image denoising methods, the characteristics of the degrading system and the noises are assumed to be known beforehand. An entire image denoising platform is provided in Fig. 3.3. The image $u(i, j)$ is corrupted by the addition of AWGN $n(i, j)$ to form the degraded image $v(i, j)$.

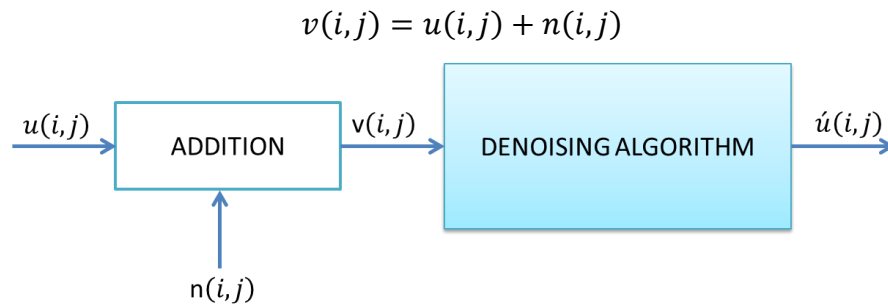


Fig 3.3 Image denoising platform

Once the corrupted image $v(i, j)$ is obtained, it is subjected to the denoising technique to get the denoised image $\hat{u}(i, j)$.

A set of two gray scale images, MRI image of human brain and CT image of abdomen, shown in Fig. 3.4, were selected for our simulations. Each image has a size of 512 x 512 and

1024 x 1024 pixels respectively with 256 shades of gray, i.e. 8 bits per pixel. In order to quantify the performance of the various denoising algorithms, a high quality image is taken and gaussian noise of known variance is added to it. This would then be given as input to the denoising algorithm, which produces an image close to the original high quality image.

The evaluation criteria are based upon quantitative measure of Peak signal to noise ratio. These measures, as such, do not represent human perception of the images, i.e. visual quality of the images. It is very difficult to gauge denoised images mathematically on visual quality as human vision system is not only highly subjective but also exhibit different tolerance levels to various types of noises. Thus authentication of denoising method requires both quantitative measure and qualitative inspection of image. In this thesis, both criterias are applied; first the PSNR and then the image is also viewed for visual acceptance.

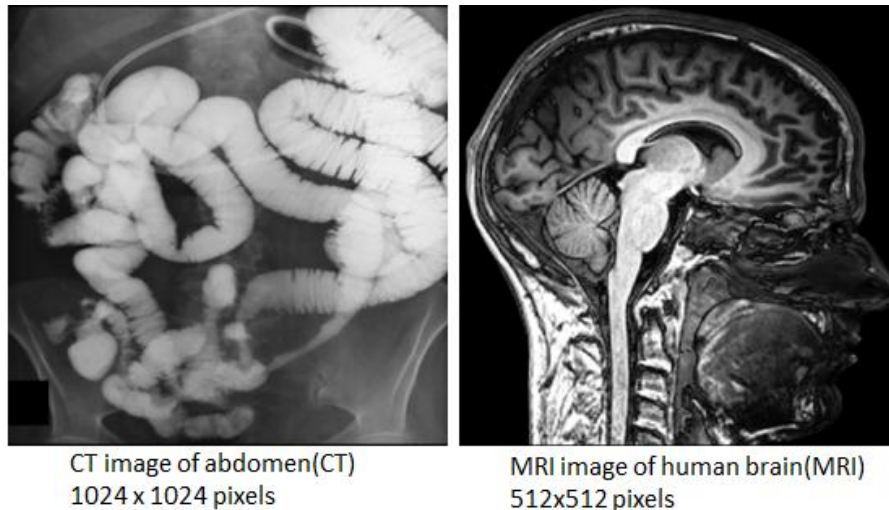


Fig 3.4 Test images

3.5 CONCLUSION

Two popular streams of denoising (transform and spatial domain methods) are studied in this thesis. Noise removal or noise reduction can be done on an image in spatial domain or transform domain. The point of focus in this project is comparing and contrasting several “medical image denoising techniques” and put forward an improved novel method of medical image denoising and also a natural image denoising scheme.

CHAPTER 4

SPATIAL DOMAIN DENOISING APPROACH (LINEAR AND NONLINEAR FILTERING)

4.1 SPATIAL DOMAIN PROCESSING

Filters play a major role in the image restoration process. The basic concept behind image restoration using linear filters is digital convolution and moving window principle [4]. Let $u(x)$ be the input signal subjected to filtering, and $v(x)$ be the filtered output. If the filter satisfies certain conditions such as linearity and shift invariance, then the output filter can be expressed mathematically in simple form as

$$v(x) = \int u(\tau) h(x - \tau) d\tau \quad (4.1)$$

where $h(x)$ is called the point spread function or impulse response and is a function that completely characterizes the filter. The integral represents a convolution integral and, in short, can be expressed as

$$v(x) = u(x) * h(x) \quad (4.2)$$

For a discrete case, the integral turns into a summation as

$$v(i) = \sum_k u(k) h(i - k) \quad (4.3)$$

This means that the output $v(i)$ at point i is given by a weighted sum of input pixels surrounding i where the weights are given by $h(i)$. To create the output at the next pixel $i+1$, the function $h(i)$ is shifted by one and the weighted sum is recomputed. The total output is created by a series of shift-multiply-sum operations, and this forms a discrete convolution.

For the 2-dimensional case, $h(i)$ is $h(i, j)$, and Equation (3.2) becomes

$$v(i, j) = \sum_{\substack{k1 \\ k2}} u(k1, k2) h(i - k1, j - k2) \quad (4.4)$$

Values of $h(i, j)$ are referred to as the filter weights, the filter kernel, or filter mask. For reasons of symmetry $h(i, j)$ is always chosen to be of size $m \times n$ where m and n are both odd (often $m=n$). In physical systems, the kernel $h(i, j)$ must always be non-negative which results in some blurring or averaging of the image. If the coefficients are alternatively positive and negative, the mask is a filter that returns edge information only. The narrower the $h(i, j)$, the better the system in the sense of less blurring.

In digital image processing, $h(i, j)$ maybe defined arbitrarily and this gives rise to many types of filters. The weights of $h(i, j)$ may be varied over the image and the size and shape of the window can also be varied. These operations are no longer linear and do not involve convolutions. They become moving window operations. With this flexibility, a wide range of linear, non-linear and adaptive filters may be implemented.

4.2 MEAN FILTER (LINEAR FILTERING)

A mean filter [4] acts on an image by smoothing it; that is, it reduces the intensity variation between adjacent pixels. The mean filter is nothing but a simple sliding window spatial filter that replaces the center value in the window with the average of all the neighboring pixel values including itself as shown in Fig. 4.2. By doing this, it replaces pixels, that are unrepresentative of their surroundings. It is implemented with a convolution mask, which provides a result that is a weighted sum of the values of a pixel and its neighbors. It is also called a linear filter. The mask or kernel is a square. Often a 3×3 square kernel is used. If the coefficients of the mask sum up to one, then the average brightness of the image is not changed. If the coefficients sum to zero, the average brightness is lost, and it returns a dark image. The mean or average filter works on the shift-multiply-sum principle. The operation of averaging blurs out the edges of the image as shown in Fig.4.1.

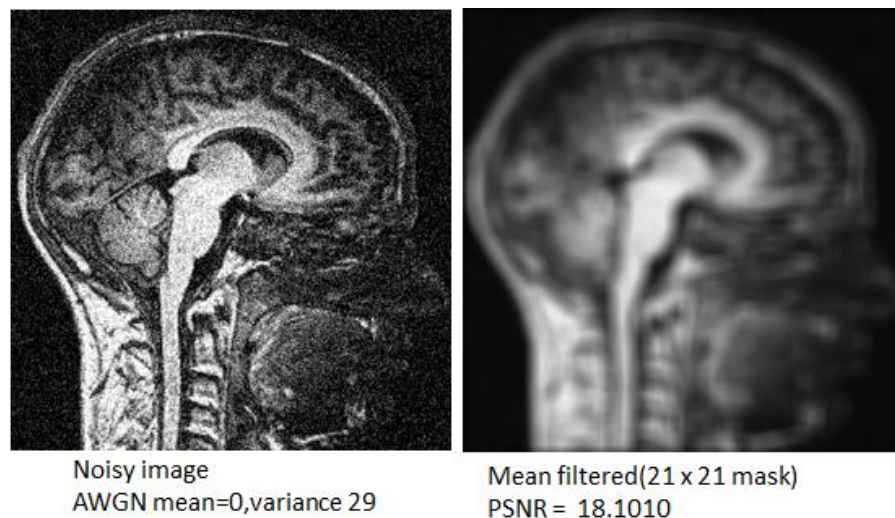
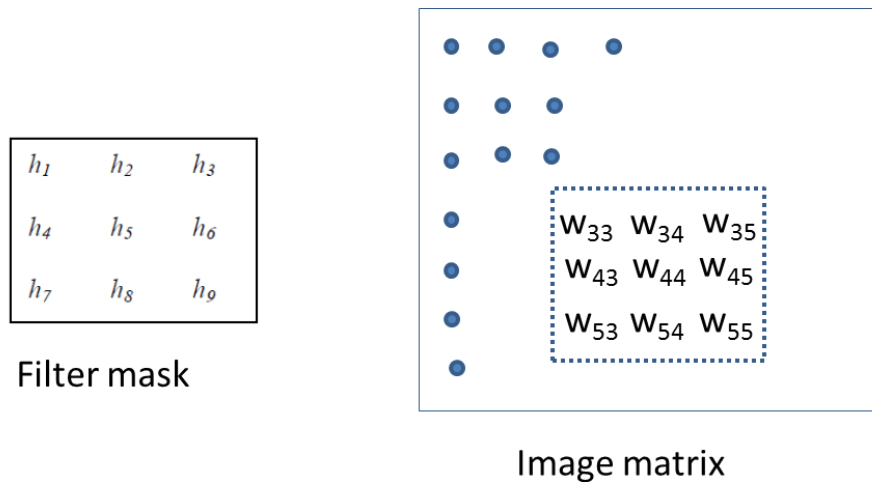


Fig 4.1 Result of mean filter



Output pixel at location (4,4)

$$= h_1w_{33} + h_2w_{34} + h_3w_{35} + h_4w_{43} + h_5w_{44} + h_6w_{45} + h_7w_{53} + h_8w_{54} + h_9w_{55}$$

Fig 4.2 Concept of mean filter

4.3 MEDIAN FILTER (NONLINEAR FILTERING)

A median filter[7] belongs to the class of nonlinear filters unlike the mean filter. The median filter also follows the moving window principle similar to the mean filter. A 3×3 , 5×5 , or 7×7 kernel of pixels is scanned over pixel matrix of the entire image. The median of the pixel values in the window is computed, and the center pixel of the window is replaced with the computed median. Median filtering is done by, first sorting all the pixel values from the surrounding neighborhood in the numerical order and then replacing the pixel being considered with the middle pixel value. Note that the median value must be written to a separate array or buffer so that the results are not corrupted as the process is performed. Figure 4.3 illustrates the methodology.

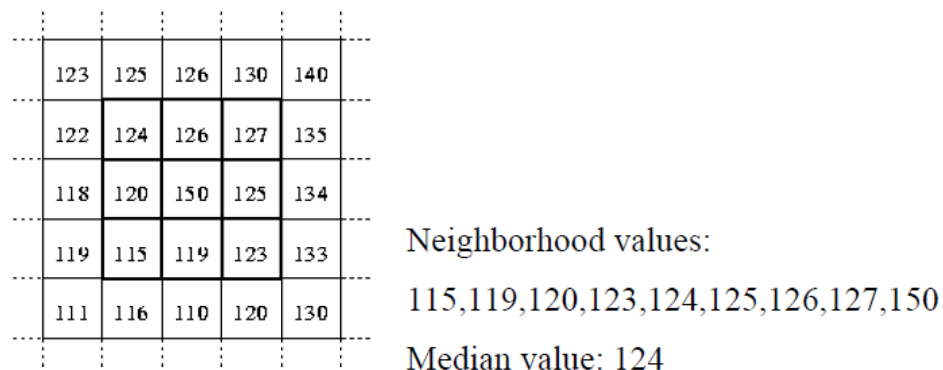


Fig 4.3 Concept of median filtering

The central pixel value of 150 in the 3×3 window shown in Fig 4.3 is rather unrepresentative of the surrounding pixels and is replaced with the median value of 124. The median is more robust compared to the mean. Thus, a single very unrepresentative pixel in a neighborhood will not affect the median value significantly.

Since the median value must actually be the value of one of the pixels in the neighborhood, the median filter does not create new unrealistic pixel values when the filter straddles an edge. For this reason the median filter is much better at preserving sharp edges than the mean filter.

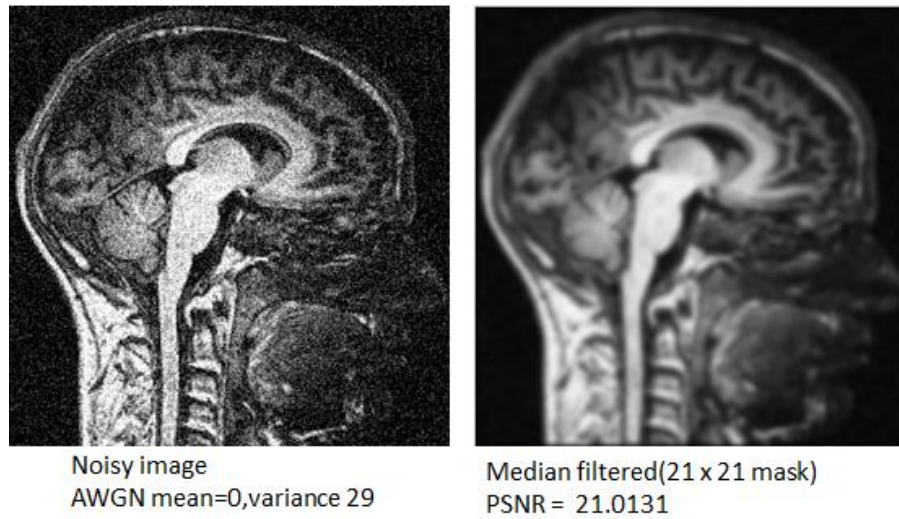


Fig 4.4 Result of median filter

4.4 BILATERAL FILTERING (NONLINEAR FILTERING)

The bilateral filter is a nonlinear filter proposed by Tomasi and Manduchi to smooth images [14,15]. The key idea of the bilateral filter is that for a pixel to influence another pixel, it should not only occupy a nearby location but also have a similar value.

The weight assigned to each neighbour decreases with both the distance in the image plane (the spatial domain S) and the distance on the intensity axis (the range domain R). Using a Gaussian G_σ as a decreasing function, and considering a gray level image I , the $BF[I]$ of the bilateral filter is defined by:

$$BF[I]_p = \frac{1}{W_p} \sum_{q \in S} G_{\sigma_s}(\|\mathbf{p} - \mathbf{q}\|) G_{\sigma_r}(|I_p - I_q|) I_q \quad (4.5)$$

Where I_p = value of image I at position: $p = (p_x, p_y)$

$F[I]$ = output of filter F applied to image I

The parameter σ_s defines the size of the spatial neighbourhood used to filter a pixel, and σ_r controls how much an adjacent pixel is down weighted because of the intensity difference. W_p normalizes the sum of the weights. The filter mask change as a function of image intensity as well as spatial location. The idea underlying bilateral filtering is to do in the range of an image what traditional filters do in its domain. Two pixels can be close to one another, that is, occupy nearby spatial location, or they can be similar to one another, that is, have nearby values, possibly in a perceptually meaningful fashion. Closeness refers to vicinity in the domain, similarity to vicinity in the range. Traditional filtering is domain filtering, and enforces closeness by weighing pixel values with coefficients that fall off with distance. Similarly, range filtering is defined, which averages image values with weights that decay with dissimilarity. Range filters are nonlinear because their weights depend on image intensity or color. The bilateral filter is also non-iterative, i.e. it achieves satisfying results with only a single pass. This makes the filter's parameters relatively intuitive since their action does not depend on the cumulated effects of several iterations. Computationally, they are no more complex than standard non-separable filters. Most importantly, they preserve edges.

On the other hand, the bilateral filter is nonlinear and its evaluation is computationally expensive since traditional methods, such as performing convolution after an FFT, are not applicable.

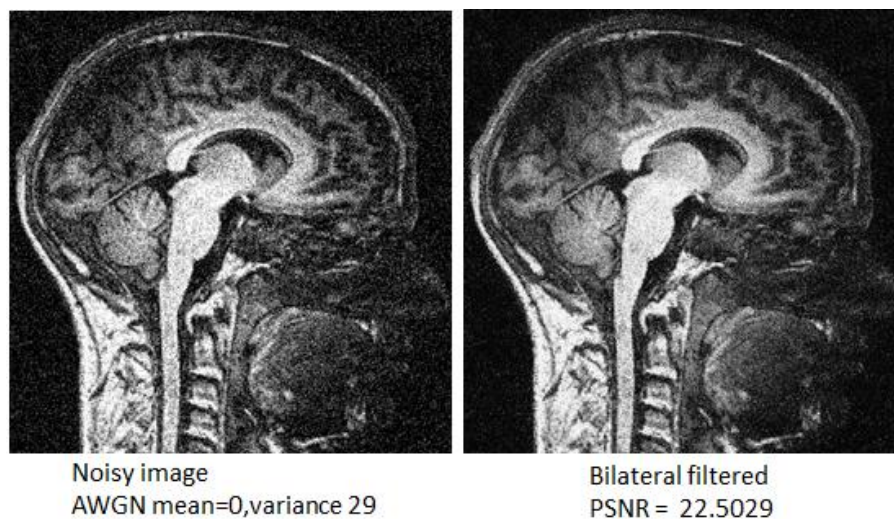


Fig 4.5 Result of bilateral filter

Many fast algorithm have been formulated for bilateral filtering ,one of the recent algorithm is formulated by Choudhary [39,40] ,which is used in this thesis.

Bilateral filtering preserves edge information after denoising. However it does not give satisfactory results, real gray levels are polluted seriously and the range filter cannot work properly. This would lead to bring side effect to the denoising results. For example, image's tissue regions may be weakened, especially small structural details and the distinct edge features. This phenomenon is referred as propagation of noise (PoN) [15].

4.5 NON LOCAL MEAN FILTERING

Buades [17,18] developed a Non-Local means (NLM) image denoising algorithm which takes full advantage of image redundancy. The basic idea is that images contain repeated structures, and averaging them will reduce the (random) noise. The NL-means filter is an evolution of the Yaroslavsky filter [22] which averages similar image pixels defined according to their local intensity similarity. The main difference between the NLmeans and this filter is that the similarity between pixels has been made more robust to noise by using a region comparison, rather than pixel comparison and also that matching patterns are not restricted to be local. That is, pixels far from the pixel being filtered are not penalized. Given an image Y the filtered value at a point i using the NL-means method is computed as a weighted average of neighbouring pixels N_i in the image following the Eqn.(4.2)

$$NL[Y(i)]_p = \sum_{j \in N_i} w(i, j)Y(j) \quad (4.6)$$

$$0 \leq w(i, j) \leq 1 \quad \text{and} \quad \sum_{j \in N_i} w(i, j) = 1$$

where i is point being filtering and j represents any other image pixel. The weights $w(i, j)$ are based on the similarity between the neighbourhoods N_i and N_j of pixels i and j . N_i is defined as a square neighbourhood window indices centered around pixel i . Theoretically, noise filtering performed must be considered as an estimation task. Since the estimation task of weights $w(i,j)$ are computationally expensive, a large number of fast methods have been developed[41,42].

The NLM filter may suffer from potential limitations since the calculation for similarity weights is performed in a full-space of neighbourhood(Fig.4.6). Specifically, the accuracy of the similarity weights will be affected by noise. This also gives the similar phenomenon as bilateral

filtering to medical images especially image's tissue region and brain grooves may be weakened by noise.

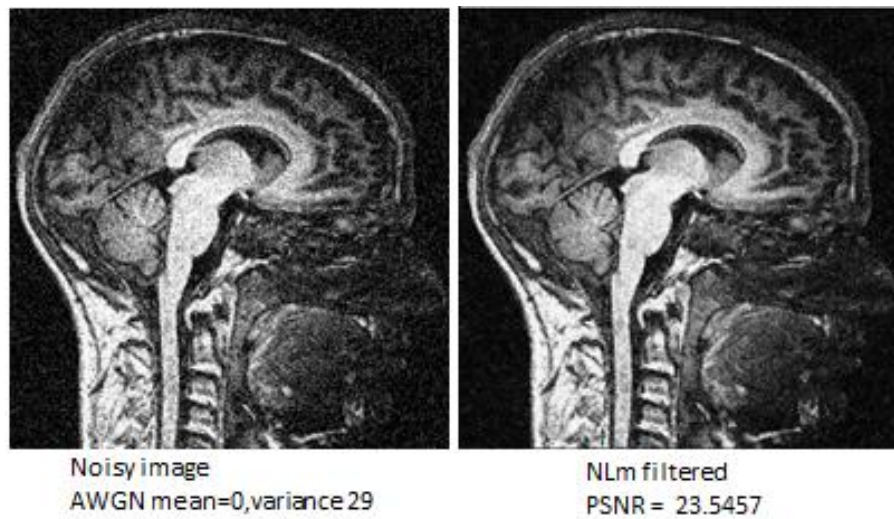


Fig 4.6 Result of NLm filter

4.4 RESULT ANALYSIS OF SPATIAL DOMAIN DENOISING

Fig. 4.7 and Table 4.1 compares different spatial domain denoising scheme.

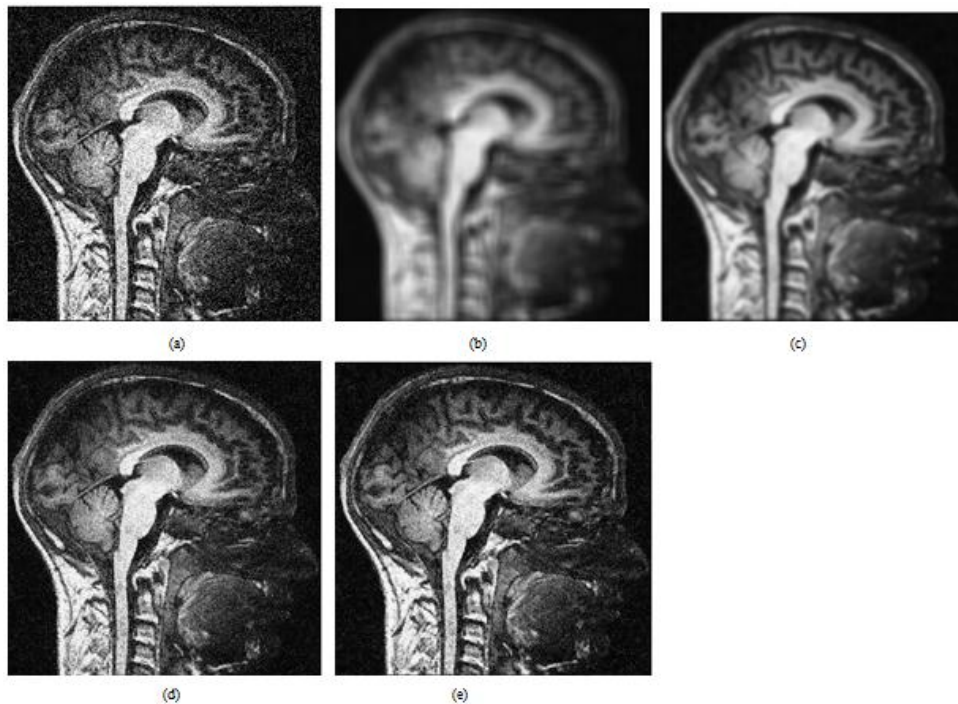


Fig. 4.7 Comparing performance (a) Noisy image ($\sigma = 40$) (b) Mean filtering (c) Median filtering (d) Bilateral filtering (e) NLm filtering.

Table 4.1 Comparing performance

Test image	Mean filtering	Median filtering	Bilateral filtering	NLM filtering
$\sigma=29$				
MRI	18.1010	21.0131	22.5029	23.5457

4.5 CONCLUSION

In this chapter we have focused on the denoising of images using the linear and nonlinear filtering techniques where linear filtering is done using the mean filter and the nonlinear filtering is performed using a median, bilateral and NLM filter. The mean filters only find applications where a small region in the noisy image is concentrated with noise. Besides, implementation of such filters is easy, fast, and cost effective. But the filtered images are blurred. The median filter provides a solution to this, where the sharpness of the image is somewhat retained after denoising. The bilateral filtering give significant improvement in conserving edges at the same time removing the noise. NLM filtering proves to be superior to bilateral filtering since it is based on structural similarity procedure. This is the reason why bilateral and NLM are used as common procedure for medical image denoising.

In spatial domain, performance of every filtering approach very much depend on the spatial intensities. For example if there is a sharp change in intensity in any of the pixel location, bilateral or NLM filter will see it as an edge and preserve it similarly to the actual edges of the image. So sudden perturbations can make the denoising algorithm based on bilateral and NLM filtering vulnerable to noise. So as a thought experiment, if we devise some preprocessing techniques prior to bilateral or NLM filter which removes the sudden discontinuities, at the same time preserving all other useful details of image, then performance of the bilateral or NLM filtering can be enhanced.

CHAPTER 5
TRANSFORM DOMAIN DENOISING
DCT,DWT AND CONTOURLET BASED DENOISING

By the application of a special transformation, an image in the spatial domain can be transformed to an equivalent form in the frequency domain. In the frequency domain each coefficient expresses a weight of a special basis function. Different transformations use different basis functions. Some of the most popular image transforms are Discrete cosine transform(DCT) and wavelet. Recently a new transform named contourlet is introduced, which is slowly emerging in every image processing applications.

5.1 DISCRETE COSINE TRANSFORM

An important and often used transformation from the spatial to the frequency domain is called the discrete cosine transform. The basis function of the DCT is the cosine trigonometric function. The DCT [4] differs from other well-known sinusoidal transformations, such as the discrete Fourier transform, in that it uses only real numbers and that different boundary conditions are implied in the frequency domain.

The most common DCT definition of a 1-D sequence of length N is

$$F(u) = \alpha(u) \sum_{x=0}^{N-1} f(x) \cos \frac{\pi(2x+1)u}{2N} \quad (5.1)$$

for $u = 0,1,2,\dots,N-1$.

Since the DCT is defined simply as a weighted sum of intensities it is clear that it is a linear transformation. The DCT also has an inverse which transform a signal from the frequency domain back to the spatial domain.

The inverse transformation is defined as

$$f(x) = \sum_{u=0}^{N-1} \alpha(u)C(u) \cos \frac{\pi(2x+1)u}{2N} \quad (5.2)$$

for $x = 0, 1, 2, \dots, N - 1$.

In both equations $\alpha(u)$ is defined as

$$\alpha(u) = \begin{cases} \sqrt{\frac{1}{N}} & \text{for } u = 0 \\ \sqrt{\frac{2}{N}} & \text{for } u \neq 0 \end{cases} \quad (5.3)$$

In literature, the value $\alpha(0)$ is referred to as the DC Coefficient. All other transform coefficients $\alpha(n)$ where n is nonzero are called the AC Coefficients.

Multi-dimensional DCT transformations can be achieved by successively employing the presented one-dimensional transform along each coordinate axis direction. The 2-D basis functions can be generated by multiplying the horizontally oriented 1-D basis functions with vertically oriented set of the same functions.

It is important to point out that no information is lost by taking the DCT of an image, as can be observed by the fact that immediately applying its inverse will yield the original image. In this sense the image in the spatial and the frequency domain are equivalent.

5.1.1 Properties Of DCT

This section outlines some properties of the DCT which are of particular value to image denoising applications.

1. Decorrelation- The principle advantage of image transformation is the removal of redundancy between neighboring pixels. This leads to uncorrelated transform coefficients which can be encoded independently. The normalized autocorrelation of the images before and after DCT transformation is shown in Fig 5.1. Clearly, the amplitude of the autocorrelation after the DCT operation is very small at all lags. Hence, it can be inferred that DCT exhibits excellent decorrelation properties

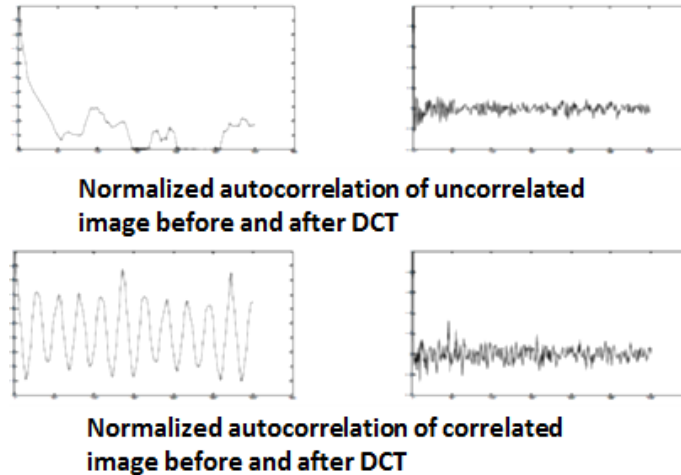


Fig 5.1 Decorrelation property

2. Energy Compaction- Efficacy of a transformation scheme can be directly gauged by its ability to pack input data into as few coefficients as possible. This allows the quantizer to discard coefficients with relatively small amplitudes without introducing visual distortion in the reconstructed image. DCT exhibits excellent energy compaction for highly correlated images as shown in Fig 5.2.

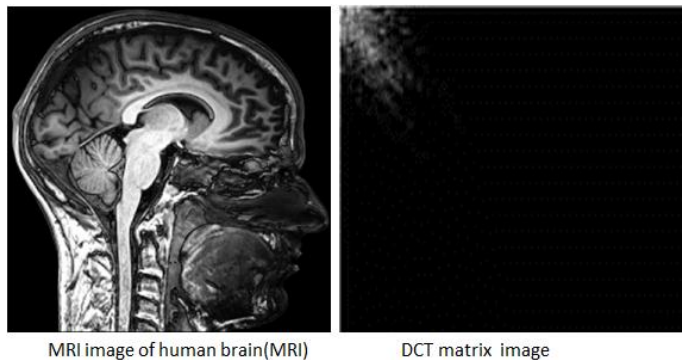


Fig 5.2 Energy compaction property

- 4 Orthogonality- In order to extend ideas presented in the preceding section, let us denote the inverse transformation of DCT matrix A as

$$IDCT = A^{-1} \tag{5.4}$$

DCT basis functions are orthogonal. Thus, the inverse transformation matrix of A is equal to its transpose i.e. $A^{-1} = A^T$. Therefore in addition to its decorrelation characteristics, this property renders some reduction in the pre-computation complexity.

5.1.2 Medical Image Denoising Using Dct Transform

It is important to point out that no information is lost by taking the DCT of an image, as can be observed by the fact that immediately applying its inverse will yield the original image. In this sense the image in the spatial and the frequency domain are equivalent. Also DCT has a strong “energy compaction” property; most of the image information tends to be concentrated in a few low-frequency coefficients in the frequency domain. Quite good approximations of the original image can be obtained even if many of the small frequency coefficients are truncated to zero before application of the inverse transform.

Considering the noise model

$$v(i, j) = u(i, j) + n(i, j) \quad (5.5)$$

Assuming the noise model as Gaussian, the magnitudes of this noise in the spatial domain is, as the name implies, Gaussian distributed and directly related to the noise variance σ^2 defined in the spatial domain.

Since the DCT is a linear operation the noisy image in the frequency domain $V(i, j)$ must be the sum of $U(i, j)$ and $N(i, j)$ as follows

$$V(i, j) = U(i, j) + N(i, j) \quad (5.6)$$

Where $V(i, j)$, $U(i, j)$, $N(i, j)$ are the corresponding DCT transform of noisy image, original image and noise image respectively.

As the biggest portion of medical images comprises of low frequency components and the high frequency portion generally consist of edges and textures, it is a reasonable assumption that the large low frequency coefficients of $V(i, j)$ will come from $U(i, j)$ and most of the small high frequency coefficients will come from the noise $N(i, j)$. This suggests that we can remove the noise of $V(i, j)$ simply by thresholding to zero its high frequency coefficients.

Often edges and rapid changes in an image are encoded in low-magnitude high-frequency coefficients and the thresholding of these to zero will result in blurring and oscillations as shown in Fig 5.3. The denoised image is both blurred and it displays an “oscillatory pattern” commonly referred to as Gibbs phenomenon [20,21]. The blurriness has the effect of smoothing out the edges. The result is an unsuccessful denoising which must come from the removal of coefficients containing “important” information.

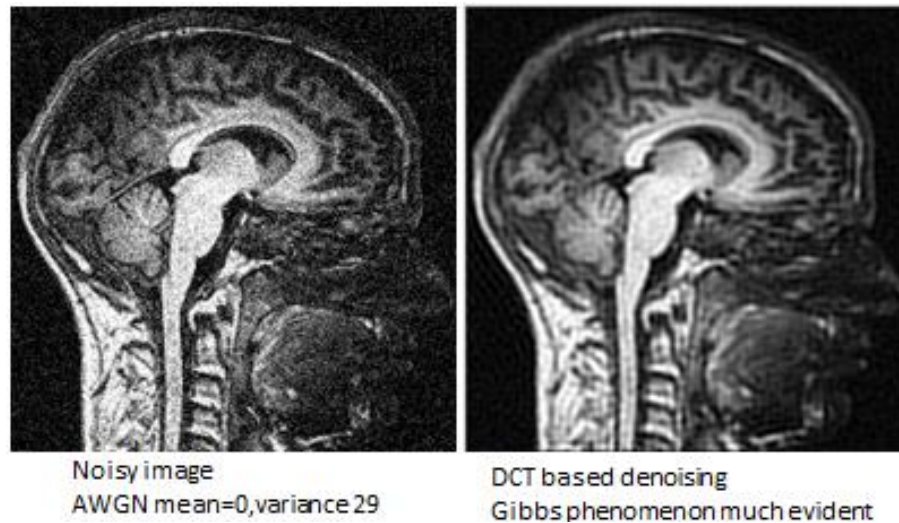


Fig 5.3 Result of DCT denoising

5.2 DISCRETE WAVELET TRANSFORM

In a discrete domain, wavelet theory is combined with a filtering theory of signal processing. The coefficients in the wavelet domain have the property that a large number of small coefficients express less important details in an image and a small number of large coefficients keep the information of significance. Therefore denoising in the wavelet domain could be achieved by killing the small coefficients which represent the details as well as the noise.

DCT representation is inadequate when it comes to analyzing transient signals. In signal and image processing, concentrating on transients (like, e.g., image discontinuities) is a strategy for selecting the most essential information from often an overwhelming amount of data. In order to facilitate the analysis of transient signals, i.e., to localize both the frequency and the time information in a signal, numerous transforms and bases have been proposed. Among those, in signal processing the wavelet is the quite standard. Also DWT is void of Gibbs phenomenon.

The central idea to wavelets is to analyze (a signal) according to scale. One chooses a particular wavelet, stretches it (to meet a given scale) and shifts it, while looking into its correlations with the analyzed signal. This analysis is similar to observing the displayed signal (e.g., printed or shown on the screen) from various distances. The signal correlations with wavelets stretched to large scales reveal gross features, while at small scales fine signal structures are discovered.

In such a scanning through a signal, the scale and the position can vary continuously or in discrete steps. The latter case is of practical interest in this thesis. From an engineering point of

view, the one dimensional discrete wavelet analysis is a two channel digital filter bank (composed of the lowpass and the highpass filters), iterated on the lowpass output. The lowpass filtering yields an approximation of a signal (at a given scale), while the highpass (more precisely, bandpass) filtering yields the details that constitute the difference between the two successive approximations. A family of wavelets is then associated with the bandpass, and a family of scaling functions with the lowpass filters.

Consider the Fig 5.4. The signal is projected into two sets of basis functions. The red box consists of a single basis shifted with respect to one another. Intuitively, that set when projected will fetch time variation of high frequency component of the signal (because basis have less duration and thus have high frequency). The band corresponds to high frequency band marked red. Similarly the blue box provides low frequency basis shifted with respect to one another and fetch low frequency portion of the signal. The band corresponds to high frequency band marked blue.

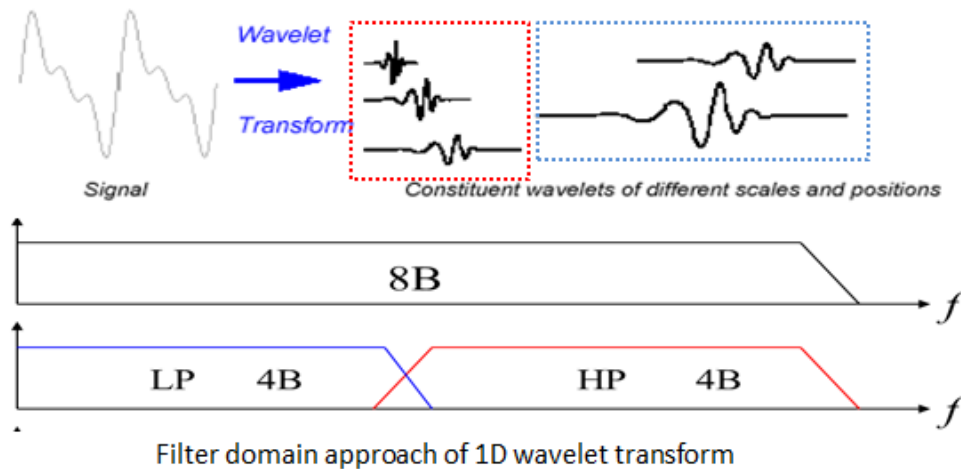


Fig 5.4 Concept of wavelet transform(two basis set)

There is no limit to this decomposition. If we found the low frequency portion have still enough energy, we can form a scaled set of the low frequency basis set and continue the process as in Fig 5.5. Same can be performed on high frequency region, if the energy is high in that region. Practically 1-D wavelet transform can be performed by passing the signal through the filterbank, which is defined by the particular mother wavelet basis and particular sets of basis used.

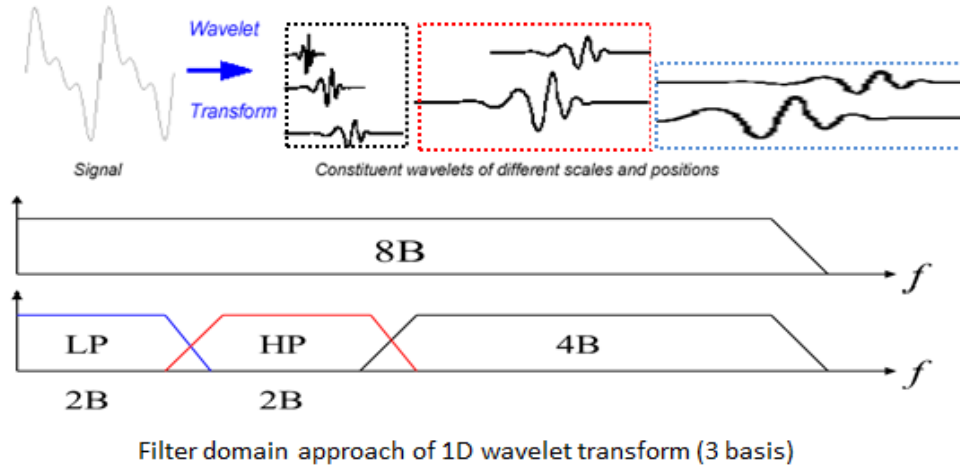


Fig 5.5 Concept of wavelet transform(three basis set)

Wavelet computation for a 2 set basis is shown in Fig 5.6. Down sampling is done on the output section to remove the redundant data, obeying with Nyquist criterion.

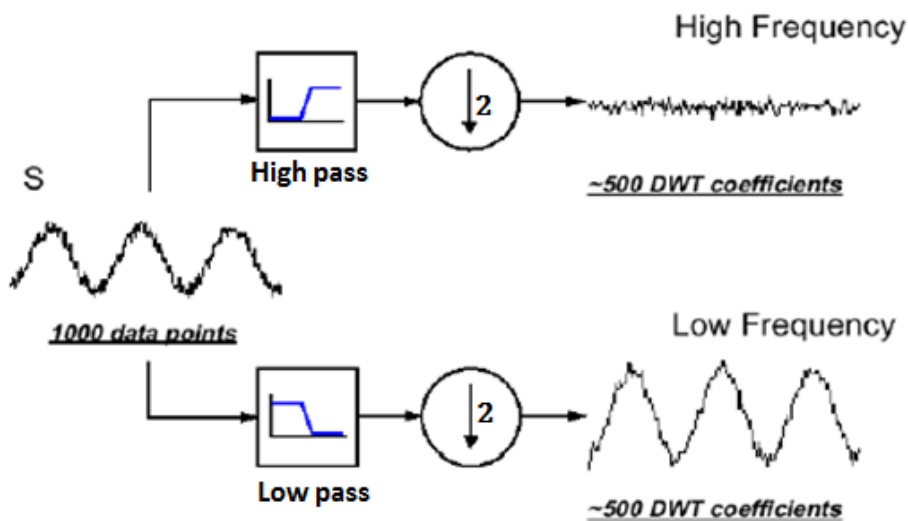


Fig 5.6 Implementation of wavelet transform(three basis set)

2-D wavelet transform can be obtained by the 1-D analysis filter bank first applied to the columns of the image and then applied to the rows. If the image has $N1$ rows and $N2$ columns, then after applying the 1D analysis filter bank to each column we have two subband images, each having $N1/2$ rows and $N2$ columns; after applying the 1D analysis filter bank to each row of both of the two subband images, we have four subband images, each having $N1/2$ rows and $N2/2$ columns. This is illustrated in the Fig 5.7.

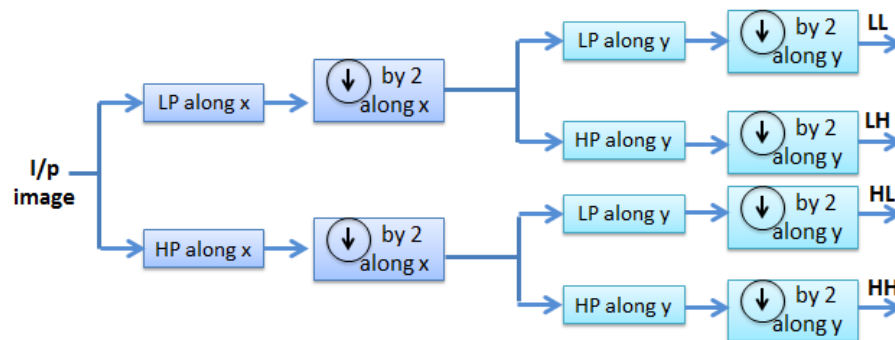


Fig 5.7 Implementation of 2-D wavelet transform

Lowpass filtering a signal give coarse details, whereas highpassing gives fine details. The subimage LL is obtained by lowpassing the image in x direction as well as lowpassing in y direction. So the resultant will be coarse details of the image. For LH, image is lowpassed in x direction and highpassed in y direction. So output will be horizontal edges of the image. Similarly HL gives vertical edges. In the case of HH, image is high passed in both directions. So the resultant will be diagonal details of the images. It is illustrated in Fig 5.8. It is also possible to again decompose the high energy subimage to further subimages. The main point to note is that, wavelet can capture only three directional details (horizontal, vertical, and diagonal).

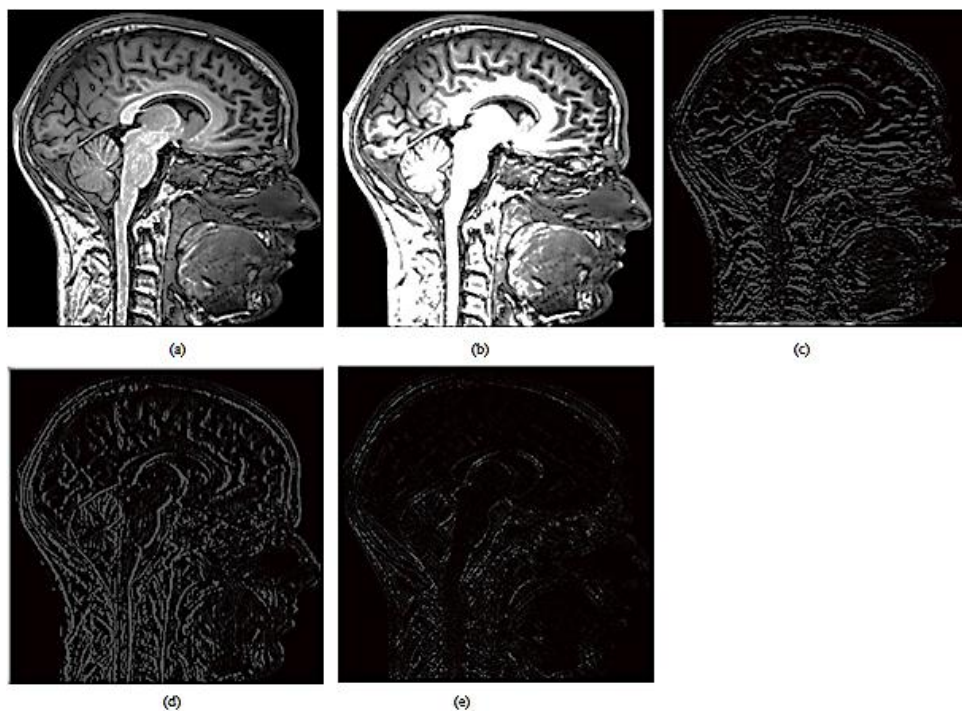


Fig 5.8 2-D wavelet transform subimage
a-Original image, b-LL, c-LH, d-HL, e-HH

5.2.1 Medical Image Denoising By Wavelet Shrinkage

The idea behind wavelet shrinkage is that Wavelet is such a basis because exceptional event generates identifiable exceptional coefficients due to its good localization property in both spatial and frequency domain[14].But considering noise, as long as it does not generate exceptions, additive white gaussian noise after WT is still AWGN.

The term wavelet thresholding(shrinkage) is explained as decomposition of the data or the image into wavelet coefficients, comparing the detail coefficients with a given threshold value, and shrinking these coefficients close to zero to take away the effect of noise in the data. The image is reconstructed from the modified coefficients. During thresholding, a wavelet coefficient is compared with a given threshold and is set to zero if its magnitude is less than the threshold; otherwise, it is retained or modified depending on the threshold rule. Thresholding distinguishes between the coefficients due to noise and the ones consisting of important signal information.

The choice of a threshold is an important point of interest. It plays a major role in the removal of noise in images because denoising most frequently produces smoothed images, reducing the sharpness of the image. Care should be taken so as to preserve the edges of the denoised image. There exist various methods for wavelet thresholding, which rely on the choice of a threshold value. Some typically used methods for image noise removal include VisuShrink, SureShrink and BayesShrink [5]. Prior to the discussion of these methods, it is necessary to discuss about the two general categories of thresholding. They are hard- thresholding and soft-thresholding types.

The hard-thresholding $H(x)$ can be defined as [22]

$$H(x) = \begin{cases} x & \text{for } |x| \geq t \\ 0 & \text{for all other region} \end{cases} \quad (5.7)$$

Here t is the threshold value. A plot of $H(x)$ is shown in Figure 5.99.

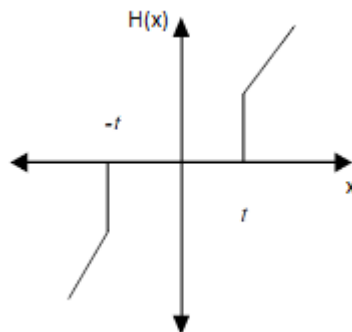


Fig 5.9: Hard thresholding

Thus, all coefficients whose magnitude is greater than the selected threshold value t remain as they are and the others with magnitudes smaller than t are set to zero. It creates a region around zero where the coefficients are considered negligible.

The soft thresholding is where the coefficients with greater than the threshold are shrunk towards zero after comparing them to a threshold value. It is defined as follows

$$S(x) = \begin{cases} \text{sign}(x)(|x| - t) & \text{for } |x| \geq t \\ 0 & \text{for all other region} \end{cases} \quad (5.8)$$

A plot of $S(x)$ is shown in Figure 5.10.

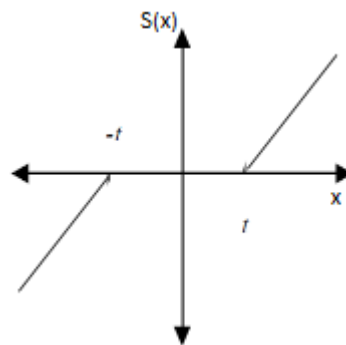


Fig 5.10: Soft thresholding

In practice, it can be seen that the soft method is much better and yields more visually pleasant images. This is because the hard method is discontinuous and yields abrupt artifacts in the recovered images. Also, the soft method yields a smaller minimum mean squared error compared to hard form of thresholding.

VisuShrink [22] is thresholding by applying universal threshold proposed by Dohono and Johnston. This threshold is given by:

$$T_u = \sigma_n \sqrt{2 \log(L)} \quad (5.9)$$

where, σ_n^2 is the noise variance of AWGN and L is the total number of pixels in an image. It is proved in [22] that a large fraction of any L number of random data array with zero mean and variance, σ_n^2 will be smaller than the universal threshold, T_U with high probability; the probability approaching 1 as L increases. Thus, with high probability, a pure noise signal is estimated as being identically zero.

For denoising applications, VisuShrink is found to yield a highly smoothed estimate and also low PSNR(Fig 5.11). This is because the universal threshold is derived under the constraint that with high probability, the estimate should be at least as smooth as the signal. So the T_U tends

to be high for large values of L , killing many signal coefficients along with the noise. Thus, the threshold does not adapt well to discontinuities in the signal.

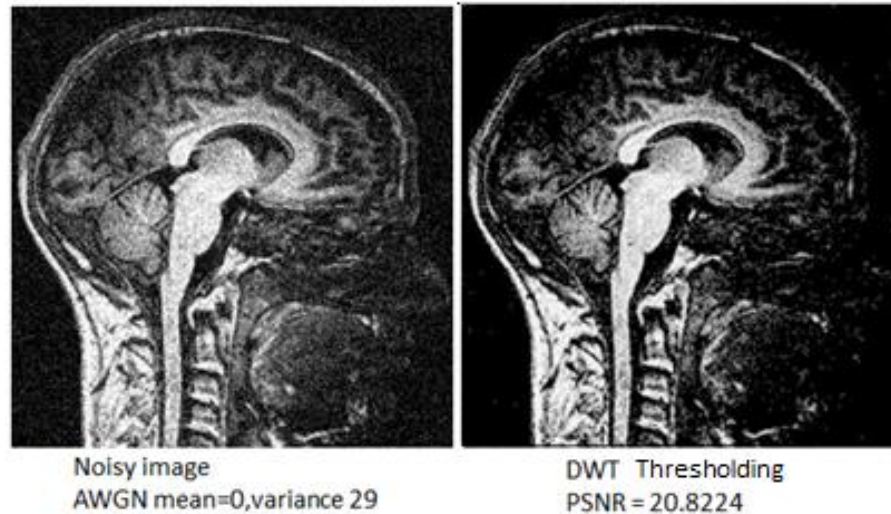


Fig 5.11: Result of wavelet visushrink

5.3 CONTOURLET TRANSFORM

The limitations of commonly used separable extensions of Fourier and wavelet transforms in capturing the geometry of image edges are discussed in the previous sections. For example, DWT can capture only three directional details.

A “wish list” for new image representations are [37]

- Multiresolution. The representation should allow images to be successively approximated, from coarse to fine resolutions.
- Localization. The basis elements in the representation should be localized in both the spatial and the frequency domains.
- Critical sampling. For some applications (e.g., compression), the representation should form a basis, or a frame with small redundancy.
- Directionality. The representation should contain basis elements oriented at a variety of directions, much more than the few directions that are offered by separable wavelets.
- Anisotropy. To capture smooth contours in images, the representation should contain basis elements using a variety of elongated shapes with different aspect ratios

Among these desired data, the first three are successfully provided by separable wavelets, while all the five satisfied by contourlet transform. For the multiresolution property, wavelet uses

further decomposition of high energy band(LL), whereas for contourlet, pyramidal filter bank is used. For the directionality property, if the transform is separable (as in wavelet), then the resultant of filtering action in both direction can fetch utmost horizontal, vertical and diagonal edges. But contourlet transform can represent more directions (more than three). So it should be a non-separable transform unlike DWT and it need to be explained with a two dimensional basis or strictly in two dimensional frequency domain. Directional filter bank gives contourlet transform the directionality property. To validate anisotropy property, for almost all separable transform, whatever we do in x directions, should be done on y direction also, It means aspect ratio of two dimensional basis of separable transform is 1:1. This is same as in the case of DWT and thus it fails anisotropy property. But contourlet transform which is a non-separable transform do not need the restriction of basis to be ratio 1:1. That is as the contourlet is strictly two dimensional, there is freedom to select transform basis of different aspect ratio. Since it is complicated to discuss contourlet in two dimensional spatial domain, it is explained in the literature strictly in frequency domain. But there is a clear connection from frequency domain and spatial domain with the use of fourier transform. For discussing contourlet transform strictly in frequency domain, we ought to explain the frequency domain counterpart of spatial domain.

5.3.1 Frequency Domain View Of Image

The mapping of time domain and frequency domain [4] is shown in fig 5.12. It is evident that different portion of different positions of frequency domain of image gives different direction.

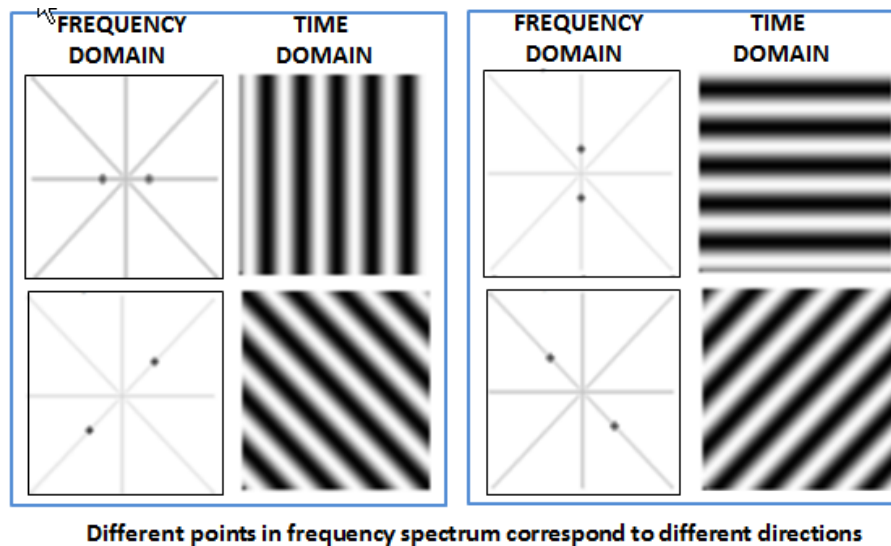


Fig 5.12 Frequency representation showing directional features

As shown in fig 5.13 ,the amplitude at the particular point of frequency domain of an image gives the intensity or brightness of directional detail correspond to that frequency point

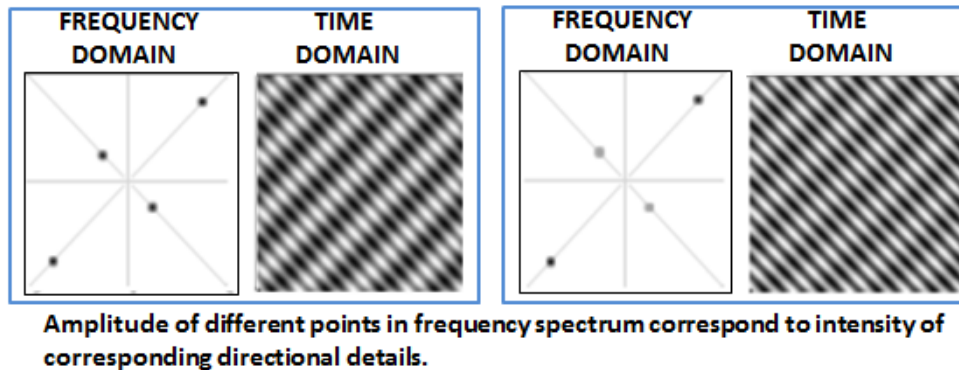


Fig 5.13 Frequency representation showing intensity of directional features

As shown in fig 5.14,if the considering point in frequency domain is near to the origin,then it represents low frequency components and if it is away from the origin,it represents high frequency component of the image.

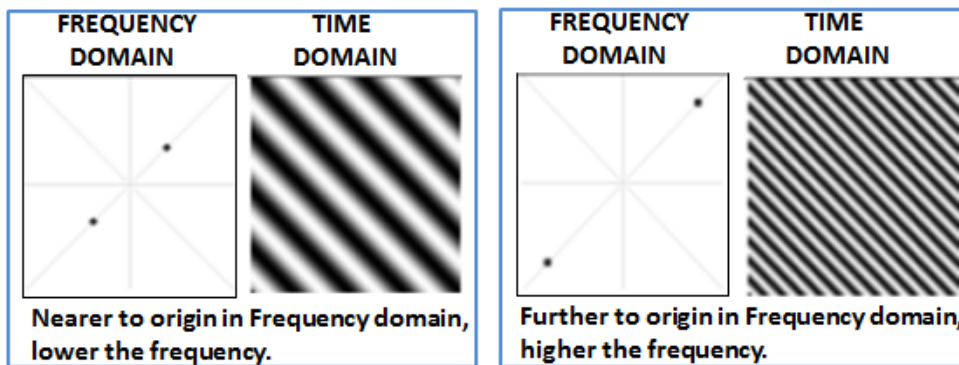


Fig 5.14 Frequency representation showing low and high frequency directional features

Decomposition is the process of separating the input image into several components, each one containing a set of frequency subbands. These sets of frequency subbands can be represented in the frequency domain by partitioning the 2D spectrum.Two filters are used to implement contourlet transform:

1. Directional Filter Bank

Fig 5.15 shows a decomposition of the frequency spectrum of the image into two, four and eight sections. Each of the components is obtained by applying a 2D filter to the image. Each section absorbs the edges corresponding to particular direction as shown in Fig 5.12 .Thus there is freedom in choosing as much section needed and thus gives contourlet transform the

directionality property. The 2D filter which captures the corresponding sections is referred as directional filter bank.

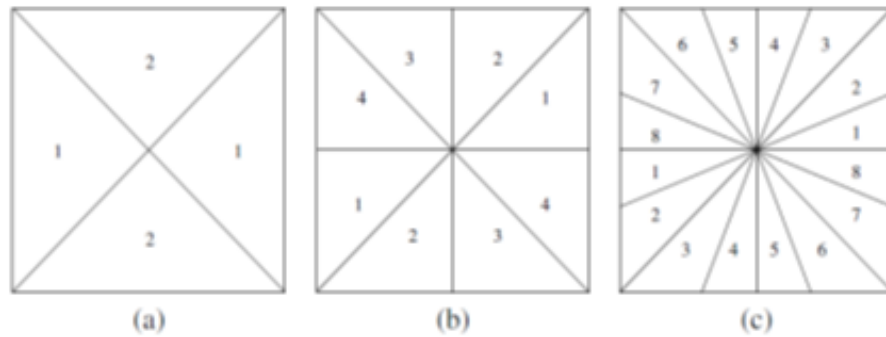


Fig 5.15: Directional filters having 2,4 and 8 bands resp.

2.Laplacian pyramid

The Laplacian pyramid (LP) as shown in Fig 5.16 is used to decompose an image into a number of orthogonal subbands. That is each band of the laplacian pyramid correspond to a definite range of frequency, thus allowing images to be successively approximated, from coarse(low frequency) to fine resolutions(high frequency).

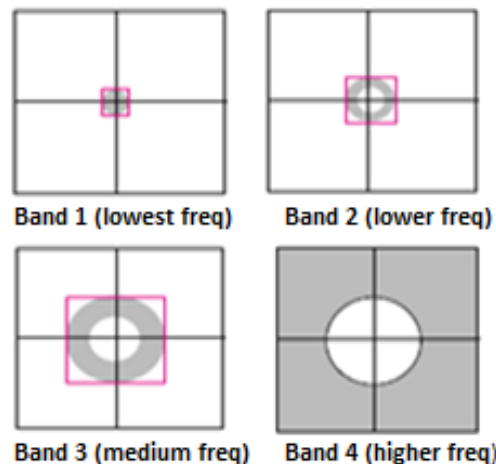


Fig 5.16 Laplacian pyramid bands

5.3.2 Construction Of Contourlet Transform

Contourlet transform is constructed using multiresolutional transform Laplacian pyramidal filter bank[43] and multidirectional transform employing directional filter bank[44](Fig 5.17). The Laplacian pyramid (LP) is used to decompose an image into a number of radial subbands, and the directional filter banks (DFB) decomposes each LP detail sub-band into a number of directional subbands. The overall result is an image expansion using elementary images like contour segments, called contourlet transform, which is implemented by a pyramidal directional filter

bank. It is also possible to again decompose high energy band (fifth subband) further to get more directional detail subbands (Similar as LL band decomposition in wavelet transform).

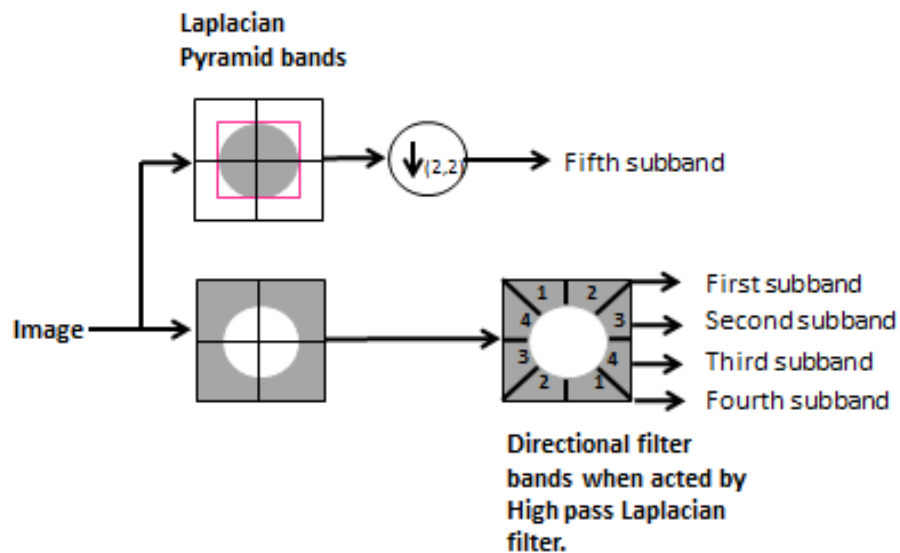


Fig 5.17 Construction of Contourlet transform

5.3.3 Medical Image Denoising By Contourlet Shrinkage

The improvement in approximation by contourlets based on keeping the most significant coefficients will directly lead to improvements in image denoising. For image denoising, random noise will generate significant wavelet coefficients just like true edges, but is less likely to generate significant contourlet coefficients.

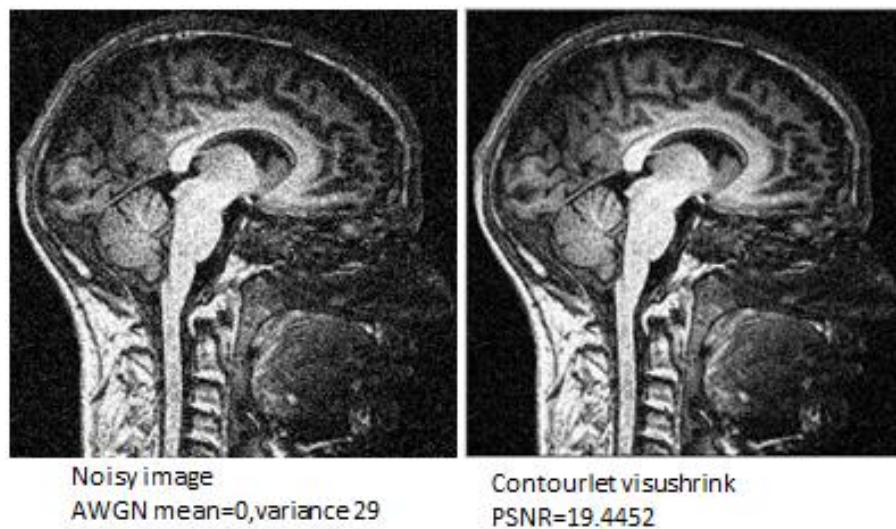


Fig 5.18 Result of contourlet thresholding

Consequently, a simple thresholding scheme applied on the contourlet transform is more effective in removing the noise than it is for the wavelet transform[37].So universal threshold proposed for wavelet can be performed to contourlet transform with the same notion. Unfortunately visushrink will not give satisfying performance for contourlet domain filtering as shown by Fig 5.18

5.4 RESULT ANALYSIS OF TRANSFORM DOMAIN TECHNIQUES

Fig. 5.19 and Table 5.1 compares different spatial domain denoising scheme.

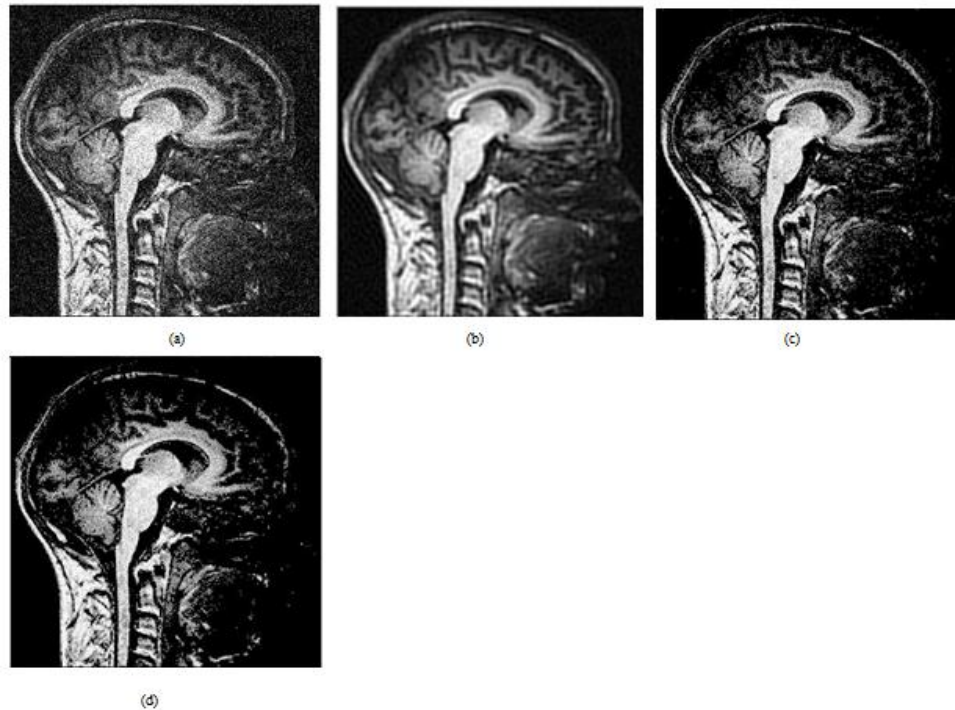


Fig. 5.19 Comparing performance (a) Noisy image ($\sigma = 40$) (b) DCT thresholding (c) DWT shrinkage(visushrink) (d) Contourlet shrinkage(visushrink).

Table 5.1 Comparison of transform domain techniques

Test image	DCT based denoising	DWT visushrink	Contourlet visushrink
MRI	21.2000	20.8224	19.4452
	Ringing effect	No ringing effect	No ringing effect

5.5 CONCLUSION

From this study it is evident that, DCT based thresholding in the frequency domain has successfully made the noisy image smoother, resulting a denoised image significantly closer to the original un-degraded image. Also observed that some of the irregularities found in the undegraded image has been removed by the denoising process. These were encoded in the small coefficients barely visible in the high frequency regions, and were truncated to zero along with the noise. For medical applications, because of ringing involved, it is not at all suitable, since many diagnosis procedures make ringing like details as false alarm.

Performance of wavelet shrinkage depends heavily on the choice of a thresholding parameter and the choice of this threshold determines, to a great extent, the efficacy of denoising. As the universal thresholding is an estimate which is asymptotically optimal in the minmax sense and universal threshold as derived by Donoho is hundred percent effective only when number of pixels in an image tends to infinity, which is an impractical situation. Also visushrink will not give satisfying performance for contourlet domain thresholding and is poorer compared to wavelet domain thresholding, even though contourlet transform is superior in terms of properties.

CHAPTER 6

PROPOSED WORK AND RESULTS.

6.1 INTRODUCTION

As the universal thresholding is an estimate which is asymptotically optimal in the minmax sense, a scaling parameter is introduced to the universal threshold by extensive simulation and regression of data with wide range of standard medical images as well as natural images of different size and corrupted by different noise variances. This idea has been extended to contourlet transformation with a new scaling factor and the same universal thresholding.

A novel medical image denoising entity is introduced using proposed contourlet thresholding as a pre-processing step prior to NLm filtering. It can give significant improvement in PSNR as well as visual quality from bilateral and NLm filter used alone. As a by-product of medical image denoising work, a novel entity is been introduced suitable for natural image denoising comprised of proposed contourlet thresholding and bilateral filtering.

6.2 NOVEL WAVELET THRESHOLDING SCHEME

Wavelet thresholding which is a signal estimation technique that exploits the capabilities of wavelet transform for signal denoising, removes noise by killing coefficients that are insignificant relative to some threshold. It turns out to be simple and effective, depends heavily on the choice of a thresholding parameter and the choice of this threshold determines, to a great extent, the efficacy of denoising. Researchers have developed various techniques for choosing denoising parameters and so far there is no “best” universal threshold determination technique. As the universal thresholding is an estimate which is asymptotically optimal in the minmax sense and universal threshold as derived by Donoho is hundred percent effective only when number of pixels in an image tends to infinity, which is an impractical situation.

Considering this delicate argument we introduce a scaling parameter to the universal threshold which is suitable for medical images whose number of pixels are finite, by extensive simulation and tabulation with different standard medical images of different size and corrupted by different noise variances. The experimental procedure adopted in this thesis is taking an

arbitrary image of known size and corrupted by a known noise variance. Then scaling factors are introduced for the universal threshold and selected the scaling factor corresponding to the highest PSNR. This procedure is repeated for large set of images of different size and corrupted by different noise variance. The compact equation of scaling parameter is obtained by linear regression of the best scaling parameter as a function of noise variance and image size.

For wavelet thresholding, tabulation and regression with different sets of medical images as well as natural images give the threshold λ_w to be

$$\lambda_w = 3.944 \times 10^{-11} S^2 - 5.5285 \times 10^{-6} S + 0.6022 \quad (6.1)$$

where S is a function of noise variance and number of image pixels, which is given as

$$S = \sigma \times \sqrt{N} \quad (6.2)$$

N is the number of pixels of the image under consideration and σ is the standard deviation of noise. So the new threshold is $T_w = \lambda_w \times T$.

The criterion for choosing S is that it should be selected as high so that percentage error which when added up due to the power terms are negligible and as low so that computational complexity for a finite word machine is at a minimum.

6.3 NOVEL CONTOURLET THRESHOLDING SCHEME

Number of transform coefficients in contourlet transform are large compared to the wavelet (in which number of transform coefficients equal to image pixels), a similar reduction in weight of coefficients take place in contourlet domain, so as to distribute values over all contourlet coefficients. So visushrink fails for contourlet transform. Therefore for contourlet thresholding, there need to be a reduction in threshold as compared to wavelet domain.

Same set of experiments done on wavelet thresholding is performed with contourlet transformation. For contourlet thresholding experimental measurements gives the threshold λ_c to be

$$\lambda_c = 3.944 \times 10^{-11} S^2 - 5.5285 \times 10^{-6} S + 0.5522 \quad (6.3)$$

where S is a function of noise variance and number of image pixels, which is given as

$$S = \sigma \times \sqrt{N} \quad (6.4)$$

where N is the number of pixels of the image under consideration and σ is the standard deviation of noise. So the new threshold is $T_c = \lambda_c \times T$. Simulation results show that proposed contourlet

thresholding and wavelet thresholding outperforms the wavelet visushrink as well as Contourlet universal thresholding .

6.4 PROPOSED MEDICAL IMAGE DENOISING ENTITY

The NLM filter may suffer from potential limitations since the calculation for similarity weights is performed in a full-space of neighborhood. Specifically, the accuracy of the similarity weights will be affected by noise. Performing contourlet denoising prior to NLM filtering can compensate noise, which can increase the accuracy of similarity weights in the full space of neighborhood and hence increase the performance of NLM filtering. Preprocessing with proposed contourlet thresholding gives better results compared to proposed wavelet thresholding because contourlet denoising is much efficient in retaining edges and texture information and hence similarity weights after thresholding.

Judging from the results, this method preserves significant edge components while denoising, which is crucial for medical image diagnosis. The proposed medical image denoising entity is shown in Fig 6.1

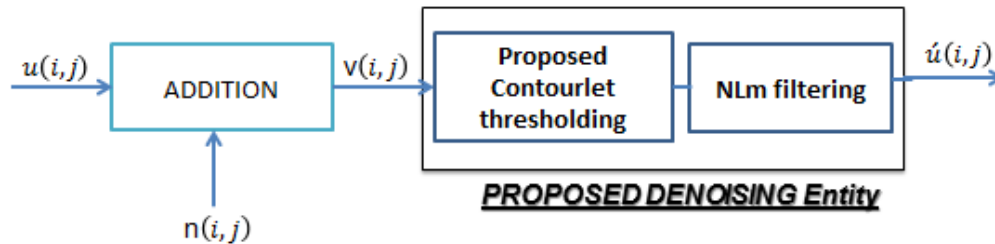


Fig. 6.1 Proposed medical image denoising entity

6.5 PROPOSED NATURAL IMAGE DENOISING ENTITY

Bilateral filtering in which real homogeneous gray levels corrupted by noise is polluted significantly, and fails to efficiently remove noise in regions of homogeneous physical properties. In homogeneous regions in which noise strike, bilateral filtering most likely perform range filtering much greater than spatial filtering. So the effect of noise is retained as if it were an edge information of the image. If contourlet denoising which is computationally efficient and having negligible execution time is done before bilateral filtering, noise in homogeneous regions which is present as un-exceptions can be removed efficiently retaining the edge information as well as texture. Simulation results show that preprocessing with proposed contourlet denoising is superior to proposed wavelet thresholding. The reason is that the only aim of the denoising prior to bilateral filtering is to remove discrepancies in homogeneous regions, but retaining edge

information and texture details as such. But wavelet transform using Visushrink smoothens the image[15] thereby degrading performance of bilateral filtering whereas contourlet thresholding is good in retaining directions and edge features.

Judging from the results, it can be verified that preprocessing bilateral filter with proposed contourlet thresholding gives a polished appearance which is aesthetic to the human eyes. The reason is due to the spatial filter in the bilateral filter. Since no spatial filtering take place in NLM filter, it fails to give the pleasing effect, which is much more important for natural images. So considering proposed contourlet thresholding and bilateral filtering as a single entity, it is highly suitable for natural image denoising, where the most important feature is pleasing to the human eyes. The proposed natural image denoising entity is shown in Fig 6.2

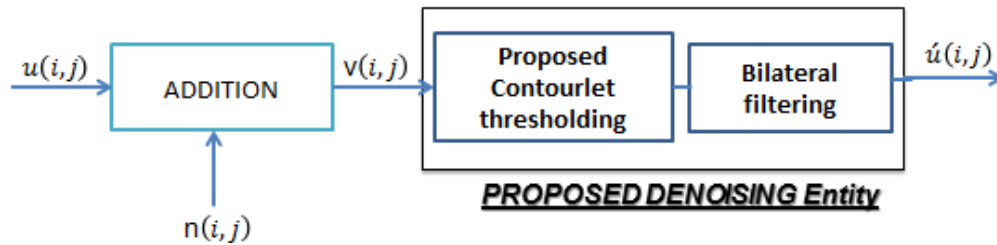


Fig. 6.2 Proposed natural image denoising entity

6.6 SIMULATION RESULTS

Table 6.1 gives the comparison of calculated PSNR of images reconstructed utilizing various thresholding. Fig. 6.3 gives the corresponding images. It is evident both visually and quantitatively that proposed thresholding scheme outperforms the existing universal thresholding schemes.

Table 6.2 gives PSNR comparison of image denoising using standard Bilateral filtering, standard non local mean filtering, and the proposed methods. Fig. 6.4 gives the corresponding images. We can see in Fig 6.4 that proposed NLM entity shows much more edges and textures, while proposed bilateral entity gives a polished appearance. So for medical image denoising where details are more important, proposed NLM entity is very much suitable.

Table 6.3 compares the processing time which is crucial for medical image processing. From the Table 6.3, it is evident that preprocessing with proposed thresholding does not increase the processing time to a much extent. Also the total processing time of the proposed entity differs from the conventional schemes upto a maximum of 0.2763 seconds.

Table 6.1 Comparison of PSNR of different thresholding schemes

Test image	Wavelet Universal Threshold	Contourlet Universal Threshold	Wavelet proposed Threshold	Contourlet proposed threshold
$\sigma = 30$				
CT	19.2590	18.0033	22.7820	23.2653
MRI	20.8224	19.4452	23.7486	23.8390
$\sigma = 40$				
CT	16.1492	14.9014	20.2541	20.7107
MRI	18.2044	16.7866	21.4390	21.5036
$\sigma = 50$				
CT	13.8143	12.6572	18.4467	18.6677
MRI	16.2471	14.8722	19.7023	19.8100

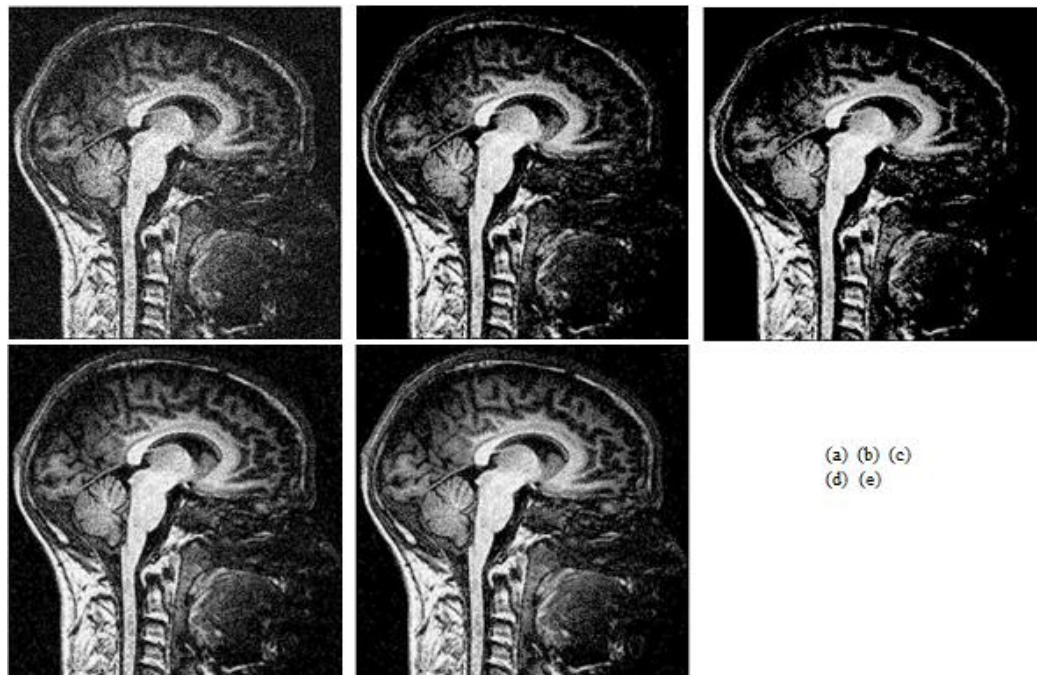


Fig. 6.3 Comparing threshold performance (a) Noisy image ($\sigma = 40$) (b)universal thresholding with wavelet (c) universal thresholding with contourlet (d)Proposed thresholding with wavelet (e)Proposed thresholding with contourlet.

Table 6.2 Comparison of PSNR of different denoising entities

Test image	Bilateral filtering	NLm filtering	Proposed preprocessing prior to bilateral filtering	Proposed preprocessing prior to NLm filtering
$\sigma = 30$				
CT	23.8733	23.9525	30.0319	30.3344
MRI	22.5029	23.5457	25.8689	26.2227
$\sigma = 40$				
CT	20.0548	19.8352	26.1260	25.1537
MRI	19.7281	20.1621	23.5916	23.5454
$\sigma = 50$				
CT	17.3835	17.1381	22.9191	22.0310
MRI	17.4913	17.6718	21.6140	21.4496

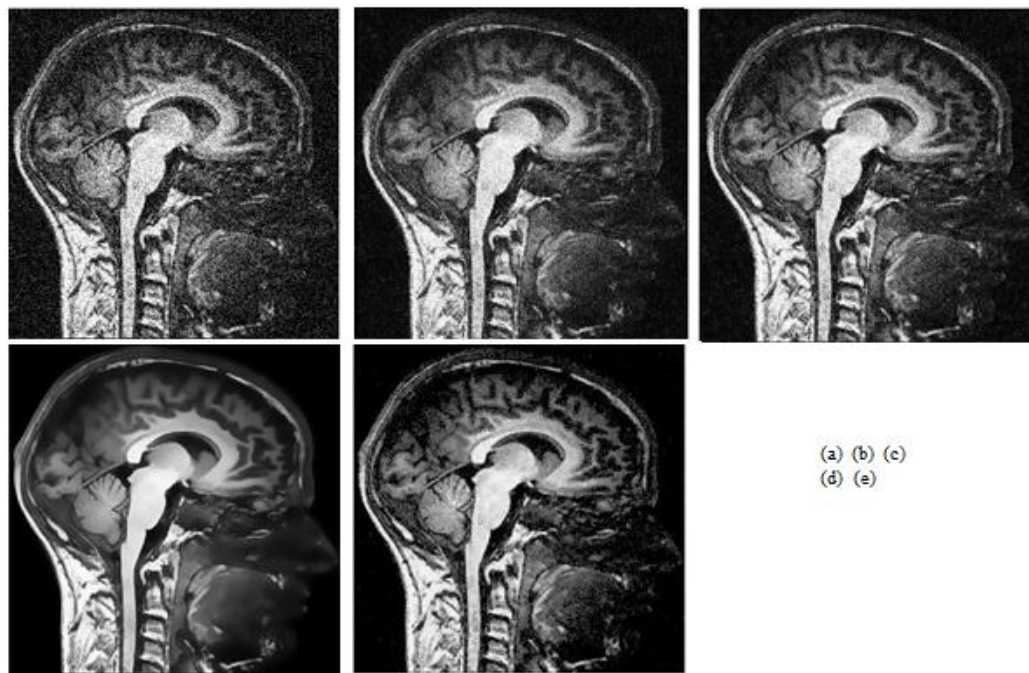


Fig. 6.4 Comparing performance of medical image denoising (a) Noisy image ($\sigma = 40$) (b)bilateral filtering (c) NLM filtering (d)Proposed preprocessing with bilateral filtering (e)Proposed preprocessing with NLM filtering.

Table 6.3 Comparison of processing time of different denoising entities
s/m specification-4 GB RAM,2.30 Ghz processor.

Test image	Bilateral filtering	NLm filtering	Proposed preprocessing prior to bilateral filtering	Proposed preprocessing prior to NLm filtering
$\sigma = 30$				
MRI	2.1578 s	2.8865 s	2.4341 s	3.0889 s
$\sigma = 40$				
MRI	2.1867 s	2.8533 s	2.3711 s	3.0183 s
$\sigma = 50$				
MRI	2.1735 s	2.8903 s	2.3639 s	3.1014 s

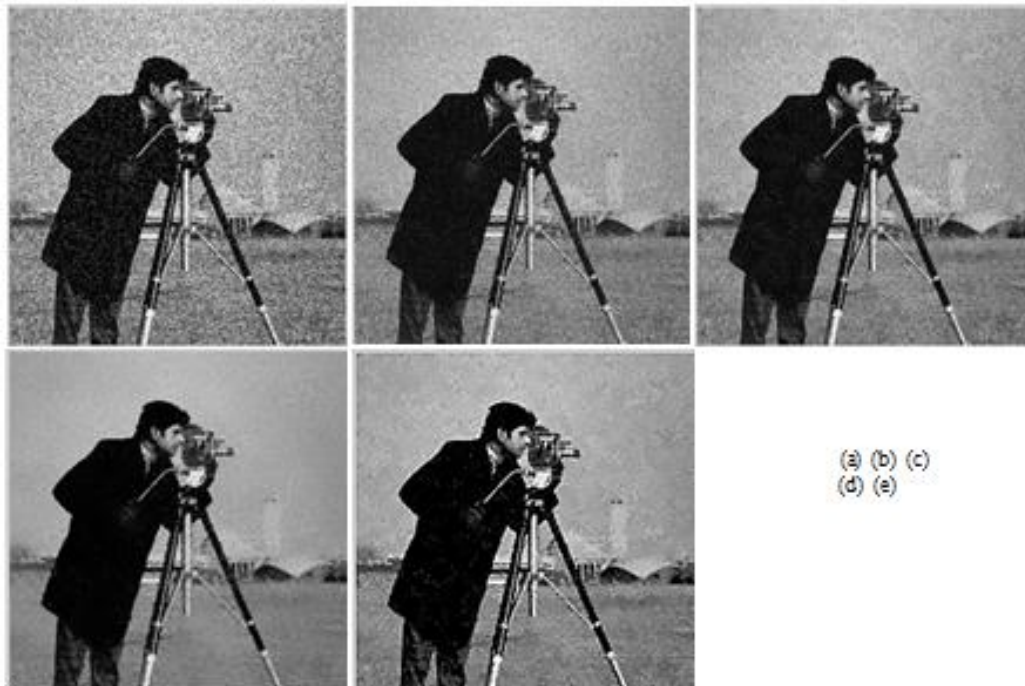


Fig. 6.5 Comparing performance of natural image denoising (a) Noisy image ($\sigma = 40$) (b)bilateral filtering (c) NLm filtering (d)Proposed preprocessing with bilateral filtering (e)Proposed preprocessing with NLm filtering.

CHAPTER 7

CONCLUSION AND FUTURE PROSPECTS.

In this work a new threshold for denoising is devised using curve fitting of best results from simulations, in contourlet and wavelet space. Contourlet transform is used here as a directional non-separable transform, to retain image textures and edges even after thresholding. The method is tested on CT abdomen and brain MRI and cameraman images. Since wavelet thresholding is cent percent effective, as the number of elements in the image tends to infinity, a novel scaling factor is been empirically formulated as a function of image size and noise variance. Also this idea is been extended to the contourlet transform. It is compared with universal threshold based on wavelet and contourlet. It is shown that for noisy images, universal threshold based on wavelet is not a proper choice. Instead we can use contourlet based methods which can retain edges in the image much better than wavelet thresholding.

An entity comprising of new contourlet thresholding as a preprocessing step prior to Non local means filtering can effectively denoise the medical images and also significantly increases the PSNR and perceptual quality as compared to Non local mean filter used alone. NLM is been selected for medical image denoising because in NLM there is no averaging of intensities take place and thus edges are effectively retained, compared to bilateral filtering which does averaging. Therefore in NLM method edges and textures are preserved effectively compared to bilateral filtering, which is more crucial for medical images.

Finally for natural images, an entity is proposed comprised of bilateral filtering and the new contourlet thresholding. Bilateral filtering is been selected since the range filtering smoothes an image to a little extent thereby giving an aesthetic value avoiding strong abnormal edge details. The denoised image obtained will be pleasing to the human eye, but fine details like edges and textures are averaged out.. The new entity gives significant improvement in PSNR compared to bilateral filter used alone.

In general as a future forethought any denoising scheme whose performance very much depend on spatial or structural features, preprocessing with proposed contourlet thresholding

happens to be a better candidate in retaining the spatial or structural features and hence enhance the performance of aforementioned denosing scheme. Also it is also possible to device a similar thresholding scheme related with a particular application by simulation and regression with large sets of data.

REFERENCES

- [1] O. Christiansen, T. Lee, J. Lie, U. Sinha, and T. Chan, "Total Variation Regularization of Matrix-Valued Images." *International Journal of Biomedical Imaging*, 2007(27432):11, December 2007.
- [2] D. Tuch, "Q-ball imaging." *Magnetic Resonance in Medicine*, 52(6):1358-1372, 2004.
- [3] S.Kalaivani Narayanan, and R.S.D.Wahidabanu, A View on Despeckling in Ultrasound Imaging. *International Journal of Signal Processing, Image Processing and Pattern Recognition*, 2009, 2(3):85-98.
- [4] Rafael C. Gonzalez, Richard E. Woods, *Digital Image processing using MATLAB*. Second Edition, Mc Graw hill.
- [5] Lu Zhang, Jiaming Chen, Yuemin Zhu, Jianhua Luo, Comparisons of Several New Denoising Methods for Medical Images. *IEEE*, 2009:1-4.
- [6] Klaus Rank and Rolf Unbehauen. 1992. An Adaptive Recursive 2-D Filter for Removal of Gaussian Noise in Images. *IEEE Transactions on Image Processing*: 431-436.
- [7] J. W. Tukey. 1974. Nonlinear (nonsuperposable) methods for smoothing data. In: *Proc. Congr. Rec.EASCOM '74*. pp. 673-681.
- [8] Hakan Güray Senel, Richard Alan Peters and Benoit Dawant. 2002. Topological Median Filter. *IEEE Trans on Image Processing*. 11(2): 89-104.
- [9] Yanchun Wang, Dequn Liang, Heng Ma and Yan Wang. 2006. An Algorithm for Image Denoising Based on Mixed Filter. *Proceedings of the 6th World Congress on Intelligent Control and Automation*. June 21-23. pp. 9690-9693.
- [10] V.R.Vijay Kumar, S.Manikandan, P.T.Vanathi, " Adaptive Window Length Recursive Weighted Median Filter for Removing Impulse Noise in Images with Details Preservation" *Electronics, And Communications Vol.6, No.1 February 2008*
- [11] S.Kalavathy, R.M.Suresh, "A Switching Weighted Adaptive Median Filter for Impulse Noise Removal" *International Journal of Computer Applications (0975 –8887)*, Volume 28– No.9, August 2011.
- [12] Zhou Wang and David Zhang, " Progressive Switching Median Filter for the Removal of Impulse Noise from Highly Corrupted Images" *IEEE Transactions on Circuits and Systems: Analog and Digital Signal Processing*, Vol. 46, No. 1, January 1999.
- [13] Rudin, L. I.; Osher, S.; Fatemi, E. (1992). "Nonlinear total variation based noise removal algorithms". *Physica D* 60: 259–268
- [14] C. Tomasi and R. Manduchi, "Bilateral filtering for gray and color images. " *Proc Int Conf Computer Vision*, pp. 839–846, 1998.
- [15] Elad, M, On the bilateral filter and ways to improve it, *IEEE Trans. On Image Processing* 11 (2002) 1141–1151.
- [16] T. Veerakumar, S. Esakkirajan, and Ila Vennila, "High Density Impulse Noise Removal Using Modified Switching Bilateral Filter" *International Journal Of Circuits, Systems And Signal Processing*, Issue 3, Volume 6, 2012
- [17] A. Buades, B. Coll, and J. M. Morel, "A review of image denoising algorithms, with a new one," *Multiscale Modeling and Simulation (SIAM Interdisciplinary Journal)*, Vol. 4, No. 2, 2005, pp 490-530.

- [18] Buadès, Antoni, Coll, Bartomeu; Morel, Jean Michel, Image Denoising By Non-Local Averaging Acoustics, Speech, and Signal Processing, 2005. Proceedings. (ICASSP '05) . IEEE International Conference on March 18-23, 2005, 25 - 28
- [19] P. Perona and J. Malik, "Scale space and edge detection using anisotropic diffusion," IEEE Trans. Pattern Anal. Machine Intell., vol. 12, no. 7, pp. 629-639, 1990.
- [20] Qingling Sun, Jinshan Tang: A new contrast measure based image enhancement algorithm in the DCT domain. SMC 2003: 2055-2058
- [21] L. P. Yaroslavsky, Digital Picture Processing - An Introduction, Springer Verlag, 1985.
- [22] D. L. Donoho and I. M. Johnstone, "Ideal spatial adaptation via wavelet shrinkage," Biometrika, 81, pp. 425-455, 1994.
- [23] J. B. Weaver, Y. Xu, D. M. Healy, and L. D. Cromwell, "Communications. Filtering noise from images with wavelet transforms," Magnetic Resonance in Medicine, vol. 21, no. 2, pp. 288-295, 1991.
- [24] C. S. Anand and J. S. Sahambi, "Wavelet domain non-linear filtering for MRI denoising,"Magnetic Resonance Imaging, vol. 28, no. 6, pp. 842-861, 2010.
- [25] Zhiling Longa, b and Nicolas H. Younana, "Denoising of images with Multiplicative Noise Corruption", 13th European Signal Processing Conference, 2005,,a1755.
- [26] Imola K. Fodor, Chandrika Kamath, "Denoising through wavlet shrinkage: An empirical study", Center for applied science computing Lawrence Livermore National Laboratory, July 27, 2001.
- [27] S. G. Chang et al., "Adaptive wavelet thresholding for image denoising and compression," IEEE Trans. Image Processing, vol. 9, pp.1532-1546, Sept. 2000.
- [28] Q Pan *et al.*, "Two denoising methods by wavelet transform," *IEEE Trans. Signal Processing*, vol. 47, pp. 3401-3406, Dec. 1999.
- [29] A. Pizurica, W. Philips, I. Lemahieu, and M. Acheroy, "A versatile wavelet domain noise filtration technique for medical imaging," IEEE Trans. Med. Image., vol. 22, pp. 323-331, Mar. 2003
- [30] J. M. Shapiro, "Embedded image coding using zerostrees of wavelet coefficients," *IEEE Trans. Signal Processing*, vol. 41, pp. 3445-3462
- [31] Y. Xu, J. B. Weaver, D. M. Healy Jr, and J. Lu, "Wavelet transform domain filters: A spatially selective noise filtration technique," *IEEE Trans. Image Processing*, vol. 3, pp. 747-758, Nov 1994.
- [32] S. Tan, L. Jio, "A unified iterative denoising algorithm based on natural image statistical models: derivation and examples", Optics Express, vol. 16 (2), pp.1056-1068, 2008.
- [33] P. Moulin and J. Liu, "Analysis of multiresolution image denoising schemes using generalized Gaussian and complexity priors", IEEE Infor. Theory, Vol. 45, No 3, Apr. 1999, pp. 909-919.
- [34] F. Russo, "Automatic enhancement of noisy images using objective evaluation of image quality", IEEE Transactions on Instrumentation and Measurement,vol. 54, no. 4, pp. 1600-1606, 2005.
- [35] A. Jung, "An introduction to a new data analysis tool: Independent Component Analysis", Proceedings of Workshop GK "Nonlinearity" - Regensburg, Oct. 2001.
- [36] A. Hyvärinen, E. Oja, P. Hoyer, and J. Hurri, "Image feature extraction by sparse coding and independent component analysis", In Proc. Int. Conf. on Pattern Recognition (ICPR'98), pp. 1268-1273, Brisbane, Australia, 1998.

- [37] Minh N. Do, and Martin Vetterli, The Contourlet Transform: An Efficient Directional Multiresolution Image Representation, IEEE Transactions On Image Processing. 2005 Page(s): 2091- 2106.
- [38] Atif Bin Mansoor, Shoab A Khann, Contoulet Denoising of Natural Images 2008 IEEE 978-1-4244-1724-7/08
- [39] Durand, F., Dorsey, J, Fast bilateral filtering for the display of high-dynamic-range images. ACM Trans. on Graphics 21 (2002) Proc. of SIGGRAPH conference.
- [40] K.N. Chaudhury, D. Sage, and M. Unser, "Fast O(1) bilateral filtering using trigonometric range kernels," IEEE Trans. Image Processing, vol. 20, no. 11, 2011.
- [41] Jin Wang, Yanwen Guo, Yiting Ying, Qunsheng Peng, Fast Non-Local Algorithm For Image Denoising, 2006 IEEE Image Processing Page(s): 1429 - 1432
- [42] Jer´ome Darbon , Alexandre Cunha, Tony F. Chan, Stanley Osher, Grant J. Jensen Rao R M and A S Bopardikar, Fast Nonlocal Filtering Applied To Electron Cryomicroscopy 5th IEEE International Symposium 2008 , Page(s): 1331- 1334.
- [43] P. J. Burt and E. H. Adelson, "The Laplacian pyramid as a compact image code", IEEE Trans. Commun., 31(4), pp. 532-540, April 1983.
- [44] R. H. Bamberger and M. J. T. Smith, "A filter bank for the directional decomposition of images: Theory and design", IEEE Trans. Signal Proc., 40(4), pp. 882-893, April 1992.